Liangliang Lin, Hue Quoc Pho, Lu Zong, Sirui Li, Nima Pourali, Evgeny Rebrov, Nam Nghiep Tran, Kostya (Ken) Ostrikov, Volker Hessel

Microfluidic plasmas: Novel technique for chemistry and chemical engineering

Chemical Engineering Journal, 2021; 417:129355-1-129355-16

Microfluidic Plasmas:
Novel Technique for Chemistry and Chemical Engineering

Liangliang Lin[1,*], Hue Quoc Pho[2], Lu Zong[3], Sirui Li[4], Nima Pourali[5], Evgeny Rebrov[2,5], Nam Nghiep Tran[2], Kostya (Ken) Ostrikov[6], Volker Hessel[2,*]

[1] The Key Laboratory of Synthetic and Biological Colloids, Ministry of Education, School of Chemical and Material Engineering, Jiangnan University, Wuxi 214122, China

[2] School of Chemical Engineering and Advanced Materials, The University of Adelaide, North Terrace Campus, Adelaide 5005, Australia

[3] School of Management, Kyung Hee University, 1 Hoegi-Dong, Seoul, 130-701, South Korea

[4] School of Chemistry and Chemical Engineering, Eindhoven University of Technology, P.O. Box 513, 5600 MB Eindhoven, the Netherlands

[5] School of Engineering, University of Warwick, Coventry, CV4 7AL, UK

[6] School of Chemistry and Physics and QUT Centre for Materials Science, Queensland University of Technology (QUT), Brisbane, QLD 4000, Australia.

* Email: linliangliang@jiangnan.edu.cn or volker.hessel@adelaide.edu.au

Abstract

As an emerging technology that features the integration of microfluidics and non-equilibrium plasmas, microfluidic plasmas not only allow the precise and effective matter and heat transport via the microfluidic system, but also provide an extremely reactive medium full of high energy plasma-generated species. Therefore, they could open new pathways for chemical synthesis or chemical engineering processes that are hardly achievable by conventional methods. In this review, three main microfluidic plasma configurations are reviewed, including plasmas confined within microchannels, plasma jets beyond microchannels and microfluidic plasma arrays. The state-of-the-art diagnostic techniques for characterizing the microfluidic plasma are also examined. A broad range of applications of microfluidic plasmas of particular interest to chemistry and chemical engineering, such as nanomaterials fabrication, prototyping, surface modification, chemical synthesis and environmental applications, are discussed. The outlook and future perspectives of this novel technology are presented.

Keywords: microfluidic plasma; microfluidics; non-thermal plasma; microplasma; microreactors

1. Introduction

1.1 Non-thermal plasmas

Being considered as the fourth state of matter, plasmas consist of highly reactive species like electrons, ions, excited molecules, radicals, and atomic species [1]. The collisions between the plasma species and other chemical compounds lead to a chemically-reactive environment, leading to the unique reaction conditions that are not accessible by traditional methods. Non-thermal plasmas are a category of plasma which is not in thermodynamic equilibrium. The selective heating of electrons by electric fields leaves the heavy particles cold [2,3]. Moreover, the collision frequency of electrons is typically 2-3 orders of magnitude larger than that of heavy particles. These energetic electrons further generate high densities of excited species or radical (metastable species) through inelastic electron-impact excitation and dissociation collisions, helping to accelerate chemical reactions and bring the processes into the otherwise hard to achieve parameter spaces [4].

The energy difference in non-thermal plasmas results in a “cold” processing condition that are

attractive for various practical applications. One of the first applications was developed by the Siemens Company for ozone generation in the second half of the 19th century [5]. Afterwards, they have been expanded onto diverse fields such as water treatment, volatile organic compounds (VOCs) decomposition, CO_2 conversion, nitrogen fixation, food preservation, surface modification, plasma medicine etc. [6–11]. For example, non-thermal plasmas can inactivate microorganisms like bacteria, cells, spores, biofilms, and viruses, making them attractive for life science fields [12,13].

Besides the above mentioned areas, large amount of research has concentrated on the non-thermal plasma-assisted nanofabrication processes, primarily driven by the unique plasma-specific effects [14]. Plasma-enhanced chemistries, in which electrons, charged particles, excited states and radicals play a role in the synthesis of nanomaterials, differ essentially from traditional approaches. Electrons or reactive species with energies of ~ eV are sufficient to initiate plasma-chemical reactions by collision with precursors, enabling reactions that are hardly achievable under typical conditions of chemical experiments [15]. These radicals also render it possible to fabricate composition-adjustable nanomaterials, with customized properties such as the size, crystallinity and morphology [16]. In addition, plasmas generate dense electron fluxes that can effectively replace chemical reductants used in wet-chemistry approaches. The rather low gas temperature further limits the aggregation of nanoparticles and meanwhile allows the use of temperature sensitive precursors [17,18].

1.2 Microfluidic technology

Microfluidics is the underlying principle of microreactor technology [19,20]. The latter enables flow chemistry [21,22] and makes it possible to utilize novel process controls [23], unusual modes of chemical operation with large disruptive potential for intensifying sustainability [24]. In commercial applications, this approach is commonly referred to as the continuous-flow processing [25], which implicitly means to make compromises when moving from the favorable micro-level to the more practical milli-level; as referred to the characteristic dimension determining the reactor performance.

Continuous manufacturing technologies produce products without ceasing. Conversely, batch manufacturing technologies produce products in a charge-wise manner, with start-up and shutdown procedures. Henry Ford’s automated assembly lines for cars are a pivotal example of continuous

production [26]. One car is made after the other – stepwise in time and space; without any stop. Continuous-flow is particularly efficient when made at a small scale, i.e., so-called microfluidics [27]. Mass and heat transfer are maximized, rendering it is possible to boost chemical production to the best performance. There are many other advantages of continuous-flow such as periodic flow patterns, (intrinsic) safety, high product quality, compact integration opportunity, and many more; see the corresponding reviews [20–22,28,29].

1.3 Generic effects by symbiosis of plasma and microfluidics

The widely acknowledged benefits of plasmas are in enhancing the reactivity of the species and accelerating chemical reactions. However, plasma operation under sub-optimal conditions may lead to excessive reaction rates and quenching of reactive species, especially at atmospheric pressure [30,31]. Additionally, non-thermal plasmas tend to be unsteady and nonuniform, caused by the lack of a topologically defined shape [32]. While efforts have been put into addressing the above issues, achieving both high conversion rates and high selectivity for conventional plasma reactors remains an unresolved problem. In this regard, reactor design in terms of size reduction and shape optimization appears to be a promising solution [33,34]

Since the early 2000s, microplasmas, the plasmas confined within submillimeter scales in at least one dimension, have been developed and gained major attention worldwide [35]. The application of microplasmas benefits from the Paschen's law which quantifies the dependence of the breakdown voltage of a discharge, for a certain gas, on the electrode spacing and the operating pressure [36]. When the plasma is confined to a smaller dimension, the breakdown voltage can be reduced, while the discharge can still be ignited and sustained at high pressure. As shown in Figure 1, the gas temperature decreases and an increase in the electron temperature can be obtained when the plasma size (electrode spacing) is reduced at a fixed pressure [37]. This phenomenon leads to the unique non-equilibrium states, which helps to expand the plasma applications. The other benefit of microplasmas is it could modify the distribution of the electric field and the charge neutrality due to the narrower electrode spacing, resulting in significant changes in the plasma properties and energy distribution of the ions, electrons, neutrals, and metastable species [38–40]. The plasma properties are closely related to

operation parameters and can differ largely with working conditions. A combined research effort involving the plasma production and diagnostic experiments complemented with numerical modeling are required to obtain the parameters of microplasmas. Due to the miniaturization effects, microplasmas possess unique properties compared to bulk plasmas, making them indispensable for advanced materials and devices.

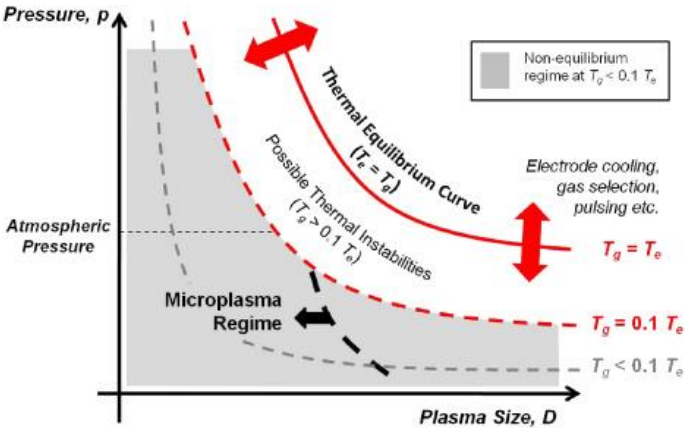

Figure 1. The relationship between the plasma pressure (p) and the electrodes spacing of plasma (D). Reprinted with permission from [37], Copyright 2010 IOP Publishing.

On the other hand, microfluidics, with its main focus on microreactors, was also parallelly introduced as an effective tool for process intensification in flow chemistry. The benefits of using microreactors include mass and energy transfer enhancements thanks to a larger ratio between their surface area and volume, the ability to safely handle toxic and explosive reactions, and flow control improvement. The idea of combining non-thermal plasma and microfluidics to form the so-called ‘microfluidic plasma’ appears to be a potential solution for process intensification and has been developed in the last few years [41]. Studies have been conducted to generate microplasma in capillaries, in microchips, in milli and micro-channels, etc., using a variety of electrodes [42].

Microplasmas are particularly promising for chemical processing in a microfluidic regime. Plasma operation for chemistry means, even in the favorable non-thermal plasma regime, typically raises the temperature. However, this effect is often overlooked in literature, and the temperature increase is difficult to measure or calculate. Yet a temperature difference as low as 10-20°C can change the selectivity of a chemical reaction to the final product, as given e.g. for the plasma-assisted conversion of methane to value-products such as ethylene or propylene, which is prone of a large

number of unwanted side reactions [43,44]. The presence of a liquid phase also provides the basic advantage to leverage reactants, which simply cannot be vaporized to the gas phase and thus widens the chemical diversity space. In addition, plasma-reactive species can be generated at the gas-liquid interface. However, it is difficult to control these species in the plasma gas phase, e.g., hydroxyl radicals in the presence of water. Microdevices have well defined flow patterns which makes it easier to control the mass and heat transfer processes. Operating plasma in contact with the liquid phase has the advantage to utilize this effective mixing and mass transfer, and having the homogeneous catalyst evenly distributed in closed neighborhood to the plasma-activated reactive species. This is one of the key requirements for a synergistic plasma catalysis [45–47]. Microfluidic plasmas can thus be suitable for liquid-phase applications beyond the synthetic chemistry such as formulations, extraction, emulsions, etc., and represent a new research area at the interface of microfluidics and plasma technology.

2. Microfluidic plasma reactors

For the generation of microfluidic plasmas, one should provide a certain energy to the microfluidic system to generate the plasma particles. The energy can be heat, electricity, or different types of electromagnetic radiation, such as microwaves, radio waves, light (ultraviolet light or intense visible light from a laser), X-rays and gamma rays, among which electricity is the mostly used form of energy. Currently, different types of microfluidic plasmas have been developed, with the application fields ranging from chemical analysis, nanomaterials synthesis to surface modification. The classification of the microfluidic plasmas is diverse. They can be discriminated according to the coupled power supply, such as DC, AC, RF, pulsed, and other excitations, or by the working gas such as Ar, He, O_2, N_2, air or their mixtures [48]. Here we divide the microfluidic plasmas into three main categories based on the general configurations: plasmas confined within microchannels, plasma jets beyond microchannels and microfluidic plasma arrays. This classification of the microfluidic plasmas is not rigid, since mixed cases can be designed and used.

2.1 Plasmas confined within microchannels The size of the plasma is essential to maintain the low gas temperatures at normal pressure while producing electrons featuring non-equilibrium energy

distributions. Thus, in addition to the commonly used nanosecond pulsed discharges (NPDs) or dielectric barrier discharges, volume confinement to micro-dimensions is another popular strategy to achieve atmospheric pressure operation of non-equilibrium plasmas. By reducing the plasma size to microscale and confining it within microchannels, a non-equilibrium reactive environment featuring diverse energetic plasma species is formed, without the need for expensive vacuum systems. This also helps to minimize sample volume as well as gas consumption. Under this concept, plasmas confined within microchannels are generated, which is the most widely reported structure among all configurations.

A salient configuration is shown in Figure 2(a), where a microchannel-confined plasma jet is developed to investigate the reactivity and reaction mechanisms of the plasma-produced oxygen atoms [49]. In this reactor design, two stainless steel (SS) electrodes spaced apart at 1 mm are connected to a 13.56 MHz commercial RF generator and grounded, respectively. A non-equilibrium radio-frequency driven plasma jet is generated within two quartz glass plates to form a $1\times1\times30$ mm^3 plasma volume. At the same time, standard and ^{18}O-labeled O_2 gas is incorporated into the helium plasma to treat aqueous solution with phenol as a chemical probe, and their flow rate can be adjusted accurately by mass flow controllers. The O_2 admixture of 0.6% in the helium plasma (He/0.6%O_2 gas mixture) yields a maximum O density of 8×10^{14} cm^{-3}. Therefore, the microfluidic plasma is an effective technique to produce O(aq) atoms and reactive nitrogen species (RNS) in the presence of water. Moreover, O(aq) atoms prove to be originated from the O_2 gas instead of water molecules, and then transfer into the liquid phase and react with phenol directly. Owing to the high reactivity of the oxygen species and nitrogen species in solutions, the microchannel-confined plasma jet shows potential for applications such as waste remediation or therapeutic treatments [50,51].

Besides using a plasma jet, plasma bubbles can also be generated within microchannels. The introduction of gas bubbles into liquid not only helps to form discharges within both small bubbles and liquid solution, but also can enhance the diffusion of plasma-produced chemical species at the interface between the plasma gas and liquids. Yamanishi et al. developed an atmospheric microfluidic chip to produce mono-dispersed plasma bubbles using a dielectric barrier discharge (DBD), as shown

in Figure 2(b) [39]. A couple of ITO coated glass substrates in a PDMS microchip with 100 μm gap are used as dielectric barriers. Water is filled between the ITO electrodes to evaluate the plasma discharge. Meanwhile, a helium gas flow is coupled to the system to form bubbles inside the microchannel. By applying electric power to the electrodes, DBD plasma bubbles are formed, while the size and number can be controlled by the flow rates of the gas and liquid. The production of plasma bubbles within microchannels and its transportation in the liquid phase have demonstrated. In this configuration, various kinds of gas are allowed as the working gas to combine chemical reactions within microchannels. Liquid is vaporized under the plasma effects, leading to discontinuous liquid-vapor boundaries as well as notable hydrodynamic effects. The discretized "plasma bubbles" within the microchip have characteristics of low temperature, high reactivity, and highly focused optical emission. Furthermore, water molecules are also dissociated to form chemically reactive species, such as electrons, radicals (OH·, O·, H·), hydrogen peroxide (H_2O_2), etc. Some electrons can reach energy above 10 eV, which in turn can enhance the diffusion of reactive species in the microfluidic system to increase the efficiency for promoting oxidation reactions in the water [52].

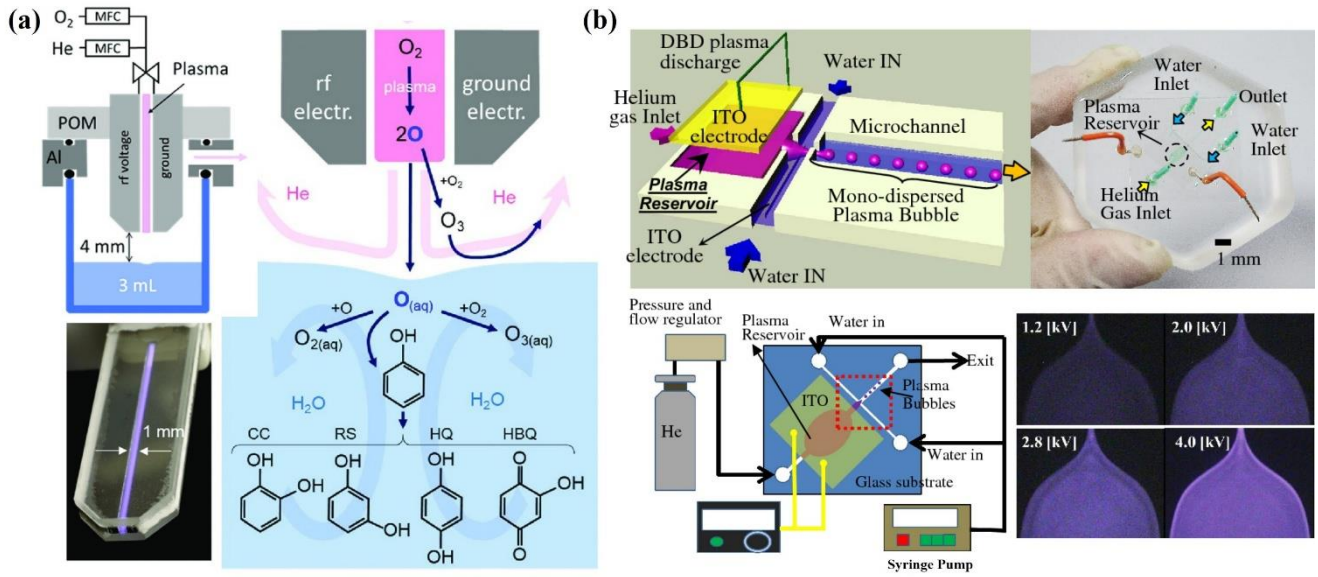

Figure 2. (a) Microchannel-confined plasma jet with He/0.6%O_2 gas mixture in operation, where the reaction pathways of O atoms in the gas phase and the phenol solution were summarized; (b) Schematic diagram of plasma bubbles formed within microchannels. Reprinted with permission from [49], Copyright 2018 PCCP Owner Societies.

2.2 Plasma jets beyond microchannels

Due to the high degree of design flexibility in the microreactor structures, the configurations of microfluidic plasmas are diverse. In this work, a specific category of microfluidic plasmas is proposed, of which the plasma jets are not confined and constrained within microchannels. Such a configuration has the key advantages including miniature geometry, high plasma density, flexible design and fast convection flow. Besides, by feeding different gases like O_2, N_2, Ar, He, H_2, CH_4, C_2H_2, organic vapors or their mixtures, the microfluidic plasma jets can be applied for the production of metals, alloys, oxides, carbides, oxycarbides, nitrides, oxynitride and polymers. Therefore, it is particularly favored by portable devices, and holds great potential for on-site chemical deposition, localized surface modifications, nanostructure growth and biomedical treatments [53]. Despite the above benefits, some gases or vapors (e.g., CH_4, C_2H_2, C_2H_5OH, $Ni(C_5H_5)_2$) might be dissociated by plasmas and lead to the clogging of microchannels. To prevent the blocking problem, the quantities of these gases or vapors should be limited. Meanwhile, operational parameters should be investigated to avoid the gas cracking.

To explore the possibility to sustain a toroidal plasmoid without applying any external electromagnetic fields, Francisco et al. introduced a microfluidic plasma jet generated at room temperature [54]. The setup consists of a ruby nozzle and a nonelectric pump. By impinging a high-speed water microjet upon a quartz wafer at velocities above 200 m/s, a plasma jet of a topologically well-defined toroidal shape is formed, with the large (toroidal) diameter of 85 μm. This is attributed to the microscale geometry in conjunction with the presence of strong electrostatic fields around the plasma jet. The confinement of plasma ions and electrons in the strong electric field leads to an intense self-induced electromagnetic field. Both the electron density (1.62×10^{17} cm^{-3}) and ionization degree (5.4%) are increased compared to bulk nonthermal plasmas. Numerical simulations show the plasma jet has a highly concentrated region of extreme strain rate, and the wall shear stress reaches ~0.5 MPa at ~66 μm from the jet axis (Figure 3(a)).

Plasma jets beyond microchannels also have the ability for *in-situ*, real-time generation of reactive oxygen and nitrogen species (RONS). This in conjunction with their portability can inspire new concepts of microfluidic plasma devices. An emerging application is to develop lightweight portable

devices for first aid, since microfluidic plasma jets can disinfect wound surface and enhance blood clotting without tissue damage [55]. In the study of Kuo [56], a portable handheld device which generated air plasma spray was used to stop wound bleeding, where pigs were used as animal models. It is revealed that the atomic oxygen species in plasmas can accelerate the coagulation process and meanwhile function as dry disinfectant. By using the plasma spray to treat a punched wound on the pig skin, the bleeding stopped after around15 s (Figure 3 (b)). As a minor temporary side effect, the plasma treatment may cause skin reddish, but this effect disappeared in two days without any apparent side effects.

As mentioned above, the microfluidic plasma jets open pathways for many promising applications. By integration with movable platform, it is possible to perform surface modification or maskless printing of arbitrary patterns of materials on selective areas [57]. As reported by Marc et al. [58], a microfluidic plasma jet integrated with a 3-axis motion platform is constructed for the site-selective surface functionalization of carbon electrodes (Figure 3(c)). A tungsten needle of 100 μm in diameter is fixed at the center of the nozzle as the electrode. Meanwhile, a RF voltage of 5 kV at 5 MHz is applied between the needle and the conductive platform to induce a microfluidic plasma jet. Water vapor mist is used as an ionic precursor for the hydroxylation and carboxylation of electrodes surface. It is decomposed in the plasma medium to form active species such as H_2O^+, H^+, H^*, OH^-, O^-, and OH^*. These H/O-containing functional groups further bombard the electrode to form a series of epoxyl, quinone, phenol, carboxyl, carbonyl, and lactone groups by means of C=O, O–C=O and C–OH bond arrangements. Consequently, hydrophilic carboxyl and hydroxyl bonds are created, leading to enhanced wettability and surface potential. The plasma jet in combination with a 3-axis motion stage allows the accurate modification of certain surface area without using complex photoresist masks. Therefore, the developed microfluidic plasma device provides an efficient and easy-to-implement way for site-selective patterning of specific surface with oxygen functionalities. Results show that after plasma treatment, the O content of carbon surface increased from 3% to 27%, while the C:O ratio decreased from 35 to 2.75. Furthermore, the hydrophilicity as well as the electrochemical properties

are improved, with a contact-angle change from ~90° to ~20°, and an significantly improvement (5-fold) in specific capacitance (from 8.82 mF·cm^{-2} to 46.64 mF·cm^{-2}).

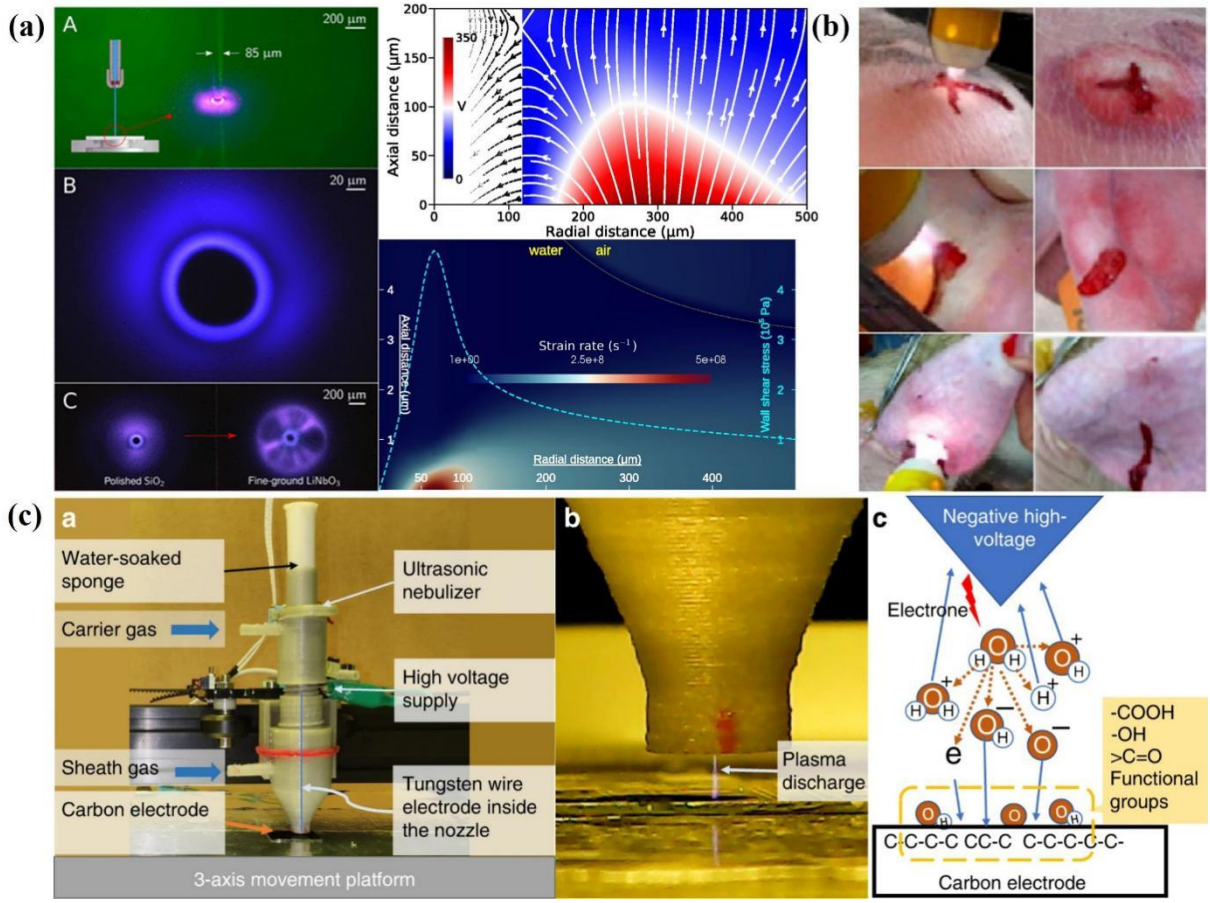

Figure 3. (a) Photograph of the toroidal plasma as well as the visual and spectral content of the plasma-radiated light through high-resolution microscopy. Reprinted with permission from [54]. Copyright 2017 PNAS; (b) The photograph of a portable plasma jet for treating a cross cut wound of pig, showing the cut is sealed around 15 s by plasma treatment. Reprinted with permission from [56]. Copyright 2016 Scientific Research Publishing Inc.; (c) An integrated system of a microfluidic plasma jet with a 3-axis platform for the surface functionalization of a carbon electrode. Reprinted with permission from [58]. Copyright 2019 Springer Nature.

2.3 Microfluidic plasma arrays

When multiple individual plasma jets are arranged in a close proximity to form an array, it can not only extend the treatment area, but also increase the throughput and efficiency of the process. As recently proposed [59], in the plasma-assisted TiN nanofabrication process, a two-dimensional plasma jet array with 100 jets in each dimension (100×100) can increase the throughput of TiN nanoparticles by four orders of magnitude. Meanwhile, the compact structure of the array design makes it only occupy a small space of ~1.5×1.5 m^2.

On the other hand, the interactions among the individual plasma jets may influence the stability of microfluidic plasma arrays. When multiple plasma jets are placed in close proximity, there are strong jet-to-jet coupling interactions caused by factors like the gas flow rates, the influence of external electric fields, the type of electrical excitation used, the magnitude of the applied voltage, etc. [60,61]. As a result, it further leads to plume divergence as well as different discharge modes, and thus affects the downstream plume uniformity and treatment effects. For practical applications like plasma-assisted surface modification or nanofabrication, the interactions among plasma jets may cause in-homogeneous surfaces or nanoparticles with undesired morphology and properties [62]. Efforts should be devoted to improve the uniformity of the plasma arrays. Therefore, there is a growing concern over the spatial and temporal uniformity and stability of large-scale microfluidic plasma arrays [63]. In the study of Kim et al [64]. a one dimensional (1D) atmospheric-pressure microfluidic plasma array consisting of 16 jets is designed to study the influence of operating parameters on the plasma behavior, such as the applied voltage, electrode configuration, pulse frequency, and gas flow rate (Figure 4(a-b)). At the optimal condition, the microfluidic plasma array exhibits high stability and uniformity while maintaining a low gas temperature. Moreover, the results of the electrical and optical emission spectra demonstrate that the array configuration can be a good candidate for delivering plasma-induced reactive oxygen and nitrogen species to the liquid, which holds great promise in cancer therapy.

In addition to the 1D array design, two dimensional (2D) microfluidic plasma arrays have also been developed. In the study of Nguyen et al. [65], a 2D array with a 9×9 microchannel plasma jet was applied for the disintegration of simulated drinking water biofilms (Figure 4(c-f)). It is suggested that at a power density of 58 W/cm^2, the exposure of the biofilm to the microplasma array for 15 min leads to the biofilm thickness to reduce from 122 ± 17 μm to 55 ± 13 μm, while more than 93% of the bacterial cells in the biofilms were killed. All the biofilms will vanish after 20 min of the plasma treatment. When the power density of the microfluidic plasma array was varied between 3.6 W/cm^2 and 79 W/cm^2, the concentrations of oxygen-bearing species were found to be in the ranges of: 85-396 nM/s for the $^1O_2$ excited molecule, 0.4-1 nM/s for the hydroxyl radicals (OH), 98-280 μM for H_2O_2

and 4-42 μM for O_3, respectively. Therefore, the microfluidic plasma arrays hold the potential to be used for the control and removal of the mixed-species biofilms through non-thermal disruption mechanisms, thus opening new opportunities for the targeted treatment of residential and commercial water systems.

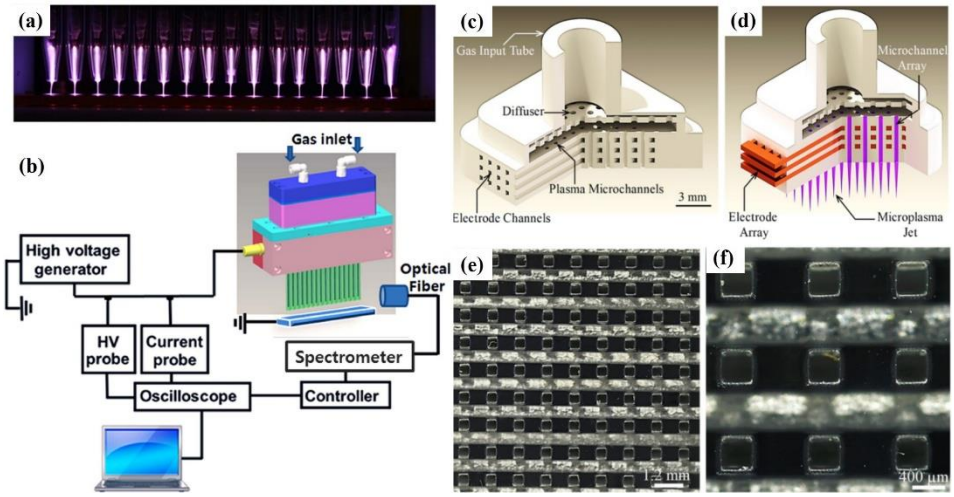

Figure 4. (a-b) The configuration and setup of the developed 1D microfluidic plasma array, with 16 plasma jets in one dimension, revealing the plasma jets have high uniformity and stability with appropriate processing parameters. Reprinted with permission from [64]. Copyright 2018 AIP Publishing; (c-d) Diagrams of the 2D microfluidic plasma array for the disintegration of biofilms in drinking water, with a 9×9 plasma jets array in two directions; (e-f) Optical micrographs of the cross-section of the 9×9 array as well as the 3×3 array confined within the microchannels. Reprinted with permission from [65], Copyright 2018 Springer Nature.

Owing to the diversity of their potential applications, the interest in microfluidic plasma arrays has risen significantly. An emerging direction is localized surface modification, where masking the sample surface or additional processing steps are not required. As a result, it provides the possibility to simplify the industrial surface engineering processes and simultaneously to avoid the use of expensive vacuum systems as well as environmentally harmful solvents [66,67]. In addition, the array configuration renders it possible to deposit coating layers with a different performance by a 2D reactor design. As described in the recent study [37], with appropriate precursors and operational parameters, multilayer functional coatings can be fabricated by scanning microfluidic plasma arrays over various substrates.

Recently, several novel microfluidic plasma arrays have been designed (as summarized in Figure 5), with numerous attempts to maximize their capacity and portability [68]. These devices do not only

reflect the versatility of microfluidic plasma configurations, but also suggest their wide applications. Regarding the scale-up behavior, when the charge is not equally distributed over the plasma jets, discharges of different energy densities might be ignited, which frequently happens due to the different gas flow rates, electrical fields, or the applied voltage among individual plasma jets. Therefore, to obtain uniform plasma arrays, uniform distribution of charge over all the jets in the array is important.

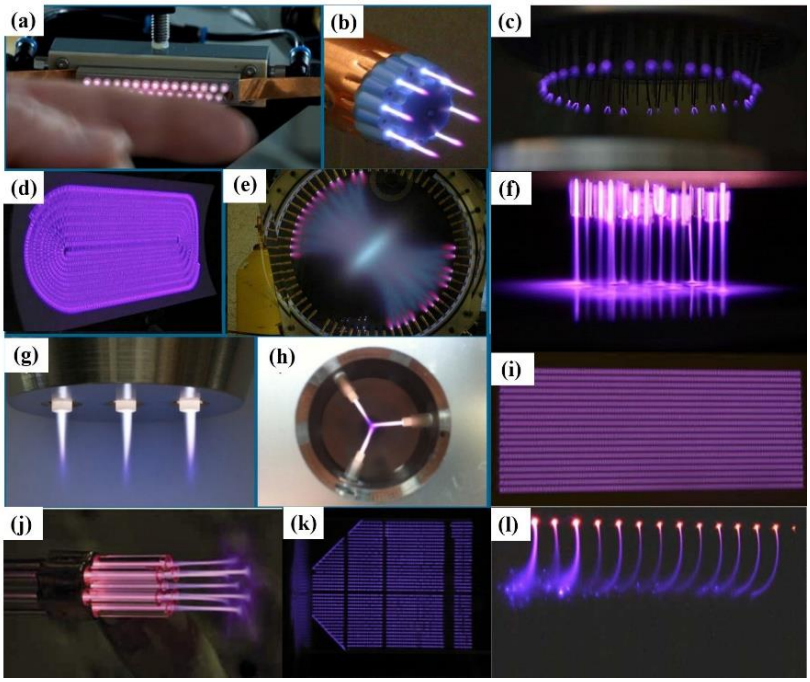

Figure 5. A summary of the reported microfluidic plasma array configurations. Reprinted with permission from [68]. Copyright 2018 IOP Publishing.

3. Diagnostics of microfluidic plasmas

Unlike organic chemistry reactions with well-defined pathway, plasmas generate a multitude of excited species and their contribution to the reaction mechanisms is complex to understand. Accordingly, the methodology and techniques of diagnostics play an essential role in the study of all kinds of plasma for chemical reactions, including the case of microfluidic plasma. In general, the diagnostic methods and techniques can be categorized into two groups: *in-situ* and *ex-situ* diagnostics. The *ex-situ* diagnostics are normally used to study the results of the plasma treatment. For example, Fourier-transform infrared spectroscopy (FTIR) or gas chromatography (GC) can be used for the analysis of gas composition after plasma exposure [69]. In the case of plasma-assisted material synthesis or surface modification, different characterization methods such as scanning electron microscope (SEM), transmission electron microscope (TEM) and X-ray powder diffraction (XRD) can

be used on the plasma-treated samples [70].

Since the plasma does not directly interfere with the measurement in the case of ex-situ diagnostics, most of the classic methods such as gas analysis or surface characterization can be applied to the microfluidic plasma process without special modification of the diagnostic procedure. On the other hand, the *in-situ* diagnostics of microfluidic plasma follows the general principles of plasma diagnostics which have been discussed in books and papers [71–73]. They could serve as good reference for this review. However, due to the small size of the channel, co-existence of gas and liquid as well as the fluidic behavior, special attention needs to be paid for the diagnostics of microfluidic plasma. Commonly used diagnostic methods including electrical diagnostics, passive and active optical diagnostics are shown in Figure 6.

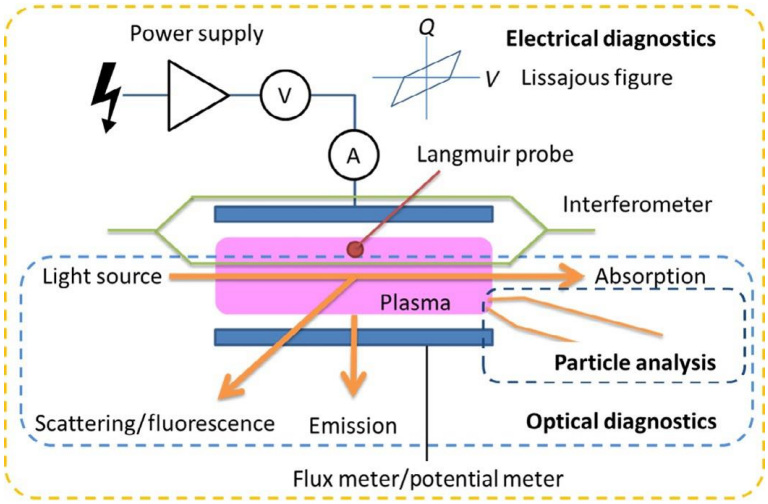

Figure 6. A summary of the common plasma diagnostic techniques. Reprinted with permission from [71], Copyright 2016 Elsevier.

The Langmuir probe has been widely used for the measurement of electron density and electron temperature in low-pressure plasmas [74,75]. However, very limited numbers of research reported the application of this method under the atmospheric-pressure microplasma conditions, since the standard collisionless theory for the Langmuir probe analysis is generally not applicable for microplasmas at high pressures [76]. In the study of Xu et. al, a high-pressure Langmuir probe developed for flames and arcs was used for the diagnostics of atmospheric microplasma jet. The electron temperature varies from 2.3 to 4 eV and the density varies from 10^{16} to 10^{19} m^{-3} depending on operation condition [77].

It should be noted that in most of the reported studies with a plasma jet, the measurement was

taken in the plume section of the jet. It will be more difficult to measure in the case of microfluidic plasma generated in a sealed microchannel. Such intrusive method is not straight forward because of the small size and the collision effect in the probe sheath region [35]. Therefore, the non-intrusive diagnostic methods such as electrical and optical approaches are preferred.

Electrical characterization mainly includes the measurement of voltage and current during the operation as well as the calculation of the power delivered. It is necessary for the monitoring and control of all plasma generated by electrical discharges. Among different types of discharges, DBD is one of the most studied plasma discharges, since it can be easily generated inside the microfluidic channel. For this type of microfluidic plasma, electrical characterization follows the general principle of plasma and more details have been explained in literature [78,79]. Voltage probes and current probes (or current transformers) have been used quite often for the measurement of electrical parameters as shown in Figure 6. It should be noted that the current probe is normally connected between the reactor and the ground to avoid the influence of possible partial discharge current outside of the reactor. Research conducted by Ogunyinka et. al developed a plasma integrated microfluidic chip based on the DBD concept, where the plasma power was measured by the Lissajous method [80].

The dynamics of the development of the microfluidic plasmas can be investigated via high-resolution photography, both in time and space. Zhang et al. [38] used a charge-coupled device (CCD) camera for the observation of flow dynamics in a plasma/liquid microreactor, and images of plasma discharge inside the reactor were captured by an intensified CCD camera to study the streamer development and propagation in electrical discharges. Another study conducted by Kim et al observed the development of plasma within the microchannel using CCD images, indicating each stage of plasma development including ignition, expansion and stable state [81]. There are also several other reported cases in which the imaging of microfluidic plasma has been involved [30,39,82].

Optical emission spectroscopy (OES) is another important technique for the diagnostics of microfluidic plasmas. Due to the simplicity and non-intrusive feature, OES has been widely used in many studies with different types of plasma discharges. The emission spectra provide important information of species generated under plasma condition, which can be further used for the analysis of

reaction condition and mechanism. Ishii et al. investigated the effect of different gas composition on the emission spectrum of plasma generated inside a microfluidic plasma reactor with adamantane by examining the CH $A^2\Delta \rightarrow X^2\Pi$ band at 431.3 nm and H_α at 656.3 nm [83]. They observed both the CH band and the H_α line appeared when H_2 was added to the mixture. By comparing this result with their previous study [84], the authors concluded that less energy is used to dissociate adamantane due to the existence of H_2 with high concentration.

Besides, OES also can be used for the investigation of plasma parameters. Toshiki et al. reported their study on spark discharges generated inside microchannels, and the electron excitation temperatures were also estimated (approximately as 2.1×10^4 K) based on the Boltzmann plot with He and Ar lines [85]. In principle, the optical diagnostics for microfluidic plasma is not significantly different compared with bulk plasmas. The general approach and techniques are the same. For example, the spectrum of the N_2 second positive system can be used to deduce the gas temperature by SPECAIR model (a program for computing, manipulating and fitting spectra) [86]; The electron density can be measured by Stark broadening of the hydrogen Balmer-β line at 486.1 nm and the electron temperature can be measured by the line ratio technique [87,88].

As a passive diagnostic method, OES only acquires the information of emitting species in the plasma. Laser-based techniques can also be very useful despite the fact that the surface scattering may occasionally cause problems [35]. Different types of laser-based techniques have been developed for the diagnosis of plasma including laser-induced fluorescence (LIF), scattering, absorption and interferometry. As suggested by Dilecce et al., LIF has been considered as a very good technique for the measurement of transient species, which offers a good combination of sensitivity, time and space resolution [89]. In addition to LIF, the scattering techniques are also very helpful to the diagnosis of microfluidic plasmas. For example, Rayleigh scattering and Raman scattering can be used to determine the gas temperature and rotational temperature respectively for molecular species and Thomson scattering can be used to determine the electron temperature and electron density in plasma [90]. Laser interferometry can also be used for the measurement of electron and gas number density in plasma with a small dimension. This technique has been applied to the diagnostics of microplasmas as

presented in several studies [91–93].

Time-resolved characterization of plasma allows detailed diagnostics of the transient plasmas. Typically, in the study of Yu et al., time-resolved laser-induced breakdown spectroscopy (LIBS) was applied for the study of the plasma properties [94]. Experimental values were processed using classical procedures based on the Stark effect, the Boltzmann and Saha-Boltzmann plot methods, revealing that the electron density and the temperatures within the plasma are functions of its decay time. Thus, by comparing the temporal evolution of the signal to noise ratio, the time-resolved LIBS technique enables the measurement of relative concentrations of ultra-trace elements with respect to a reference element.

The development of diagnostic techniques allows us to gain insight into the complicated plasma process, and provides valuable information to develop validated plasma kinetic models. In order to serve as a guidance for researchers in this field, an overview of the plasma characterization techniques is presented in Table 1 [95].

Table 1. Overview of the plasma diagnostic methods. Reprinted with permission from [95]. Copyright 2016 IOP Publishing.

Quantity	Method	Comment	Ref.
I, V	Shunt resistor, Rogowski coil, voltage dividers		[96]
P	(a) Current-voltage	(a) Used for pulsed, DC and AC discharges	[97,98]
	(b) Voltage-charge	(b) Typically used for DBD	
	(c) Thermally based power meters	(c) Used for RF and MW discharges	
n_e	(a) Stark broadening	(a) Typically H_β, $n_e > 10^{20}$ m^{-3}	[97,99–101]
	(b) Thomson scattering	(b) *In situ*, calibration necessary	
	(c) Interferometry	(c) Line of sight measurement, effect of T_g	
	(d) Continuum radiation	(d) Absolute calibration necessary	
T_e	(a) Thomson scattering	(a) In situ (electron energy distribution function (EEDF) remains a challenge)	[99–102]
	(b) Line intensity ratio rates only available for limited gas mixtures	(b) Need of collisional radiative model, reaction	
	(c) Continuum radiation	(c) Absolute calibration necessary	
T_g	(a) Rotational emission spectra	(a) Non-equilibrium effects possible	[103,104]
	(b) Rotational absorption spectroscopy	(b) Ground state diatomic molecule	
	(c) Rotational LIF spectra	(c) Ground state diatomic molecule	
	(d) Rotational Raman Scattering	(d) Ground state diatomic molecule	
	(e) van der Waals broadening	(e) Atomic line with small Stark broadening at low gas temperatures	
	(f) Doppler broadening	(f) Atomic line with small Stark broadening at elevated gas temperatures	
	(g) Rayleigh scattering	(g) Gas density measurement, species dependent	
	(h) Schlieren imaging	(h) Refractive index measurement	
	(i) Thermal probes	(i) Possible interactions of plasmas with probe	
E/N	(a) $N_2(C)$ /$N_2^+(B)$ ratio	(a) Electron excitation should be dominant	[105,106]
	(b) Coherent anti-Stokes Raman scattering (CARS)	(b) Performed in H_2 and N_2 containing gases	
H_2O	(a) Absorption	(a) Line integrated measurement	[107–109]
	(b) Raman scattering	(b) Spatially resolved but less sensitive	
	(c) OH LIF (quenching measurement)	(c) Other gas molecules determine detection limit	
N_2,O_2	(a) Raman scattering	(a) Spatially resolved	[110,111]
	(b) Mass spectrometry	(b) Sampling only at solid interface	
O•, N•, H•, …	(a) TaLIF	(a) Requires calibration and quenching corrections	[112,113]
	(b) Vacuum ultraviolet (VUV) absorption	(b) Requires VUV wavelengths which are absorbed in O_2, H_2O	
	(c) Mass spectrometry	(c) Sampling only at solid interface, interferes with cracking patterns from internal MS ionization source	
•NO, •OH,	(a) LIF	(a) Requires calibration	[114]
	(b) UV absorption	(b) Line integrated measurement	
	(c) Mass spectrometry	(c) Sampling only at solid interface, interferes with cracking patterns from internal MS ionization source	
Ar_m, He_m, $N_2(A)$	(a) LIF	(a) Requires calibration by eg. Rayleigh scattering	[115,116]
	(b) Diode laser absorption	(b) Line integrated measurement	
(H)$NO_x^{(-)}$, H_2O_2,	Multi-pass absorption (FTIR)	Line integrated measurement	[117,118]
Positive ions	(a) Mass spectrometry	(a) Sampling only at solid interface	[119,120]
	(b) LIF	(b) Only particular ions such as Ar^+, N_2^+have been studied	
Negative ions	(a) Mass spectrometry	(a) Sampling only at solid interface	[121]
	(b) Photo-detachment	(b) Requires absolute determination of n_e	

4. Applications of microfluidic plasmas in chemistry and chemical engineering

The reduction of plasma size to micrometer dimensions not only leads to unique physical properties (e.g., enhanced plasma chemistry, strong gradients, extreme thermal non-equilibrium), but also provides unprecedented access to a largely unexplored operational windows that are not achieved by traditional methods. For example, the combination of plasma with microreactors makes it possible to integrate energy in the form of electrochemical, hydrothermal, photo-driven and microwaves. At the same time, diverse reaction media such as gaseous, liquid, solid and mixed-phase media can be generated. These characteristics may be instrumental to deliver technological impact across several scientific and socio-economic domains. In this section, salient examples of microfluidic plasmas applications are illustrated.

4.1 Nanomaterials fabrication

Despite nanomaterials having received great attention in numerous fields, they may induce dangerous effects in living organisms, since conventional chemical approaches for preparing nanomaterials require toxic reducing agents or oxidants [122]. Therefore, an alternative toxic-chemical-free synthesis is essential for the development of nanobiotechnology and other fields. In the past five years, microplasma-assisted nanofabrication of functional nanomaterials such as iron oxides [123], nickel nanoparticles [124], titanium nitrides [59], yttrium nanoparticles [125], lanthanide doped yttria nanophosphors [126,127], N-doped carbon dots (N-CDs) [128], has been demonstrated.

The innovative idea of combining non-thermal plasmas and microfluidics offer a new pathway to prepare functional nanomaterials continuously and controllably. For examples, in the study of Mariotti et al. [129], a non-thermal plasma jet confined within a quartz capillary is applied for the gas-phase synthesis of Sn nanocrystals. Helium is selected as the plasma gas, and the gas flow rate is adjusted in the 0.25-1 standard litre per minute (SLM) range to control the residence time of the precursors. By regulating the operational parameters such as the gas flow rate, gas composition and plasma power, their effects on the products are investigated. Surfactant-free, ultrasmall, free-standing Sn nanocrystals of high crystallinity and purity are synthesized by the capillary-confined plasma jet. Moreover, the designed microfluidic plasma allows accurate control on the size, morphology, and crystal structures

of the products by tuning operational parameters. The obtained Sn nanoparticles (NPs) also prove to possess excellent electrochemical capacity for energy storage devices such as microsupercapacitors.

In addition to gas-phase synthesis of nanomaterials, microfluidic plasmas are also very attractive for nanofabrication in the liquid phase. The plasma-liquid interaction generates chemically reactive species at the interface, such as e^-, ·NO, O·, ·OH, H·, H_2O_2 and ·HO_2. Some of the generated reactive species in the gas phase will move to the liquid surface by diffusion and convection [130]. For example, free electrons can enter into the solution to form hydrated electrons (e^-_{aq}), with an average penetration depth of 12.3±4.9 nm [131]. Simultaneously, some species may desorb from the liquid phase and enter the gas phase through quite similar processes. Since the plasma generally transfers heat to the liquid surface, vapors will be produced from the liquid and evaporate at the gas-liquid interface. This is always associated with the energy transferred to or from the liquid surface.

Figure 7(a) shows schematics of temperature and concentration profiles in the plasma-liquid interface [95]. In terms of the plasma chemistry, chemically reactive species are formed at the interface when plasma gets in contact with water, where the dehydrated electrons have the strongest reducing ability for most of the ions in the solution. Importantly, when plasma is removed, plasma-assisted chemical reaction can be ended immediately without generating reductant residuals. Li et al. (2018) used a DBD microfluidic plasma to synthesize gold nanoparticles, which is shown in Figure 7(c) [132]. Instead of using chemical reductant, electrons from helium plasma are used as the reducing agent to reduce Au^{3+} ions.

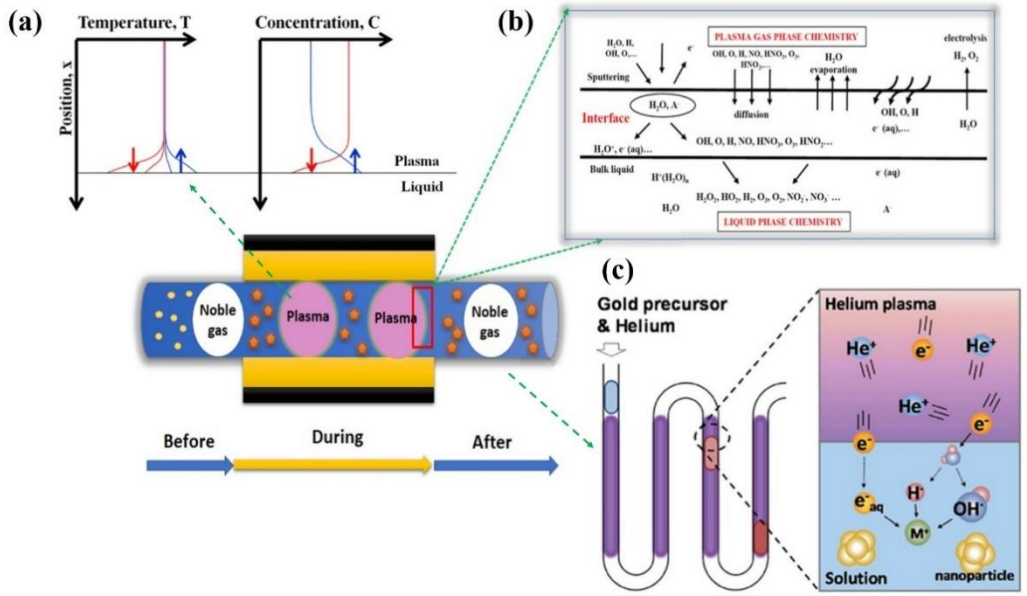

Figure 7. The synthesis of AuNPs by a microfluidic plasma reactor: (a) Temperature and concentration profiles in the plasma-liquid interface. The arrows indicate that both plasma species and heat can be transported in either direction. Reprinted with permission from [95], Copyright 2016 IOP Publishing; (b) The most important species and mechanisms of plasma in contact with water; (c) Au^{3+} reduction and gold nanoparticle synthesis using plasma confined within microchannel. Reprinted with permission from [132], Copyright 2018 The Royal Society of Chemistry.

Besides the above advantages, microfluidic plasma for nanofabrication allows for the use of a various precursors, which can be supplied as gases, liquids, or even solids (like nanoparticles), as long as they will not block the microchannels. These advantages have enabled the impressive tunability in terms of the reactor design, operation process, product composition and structure.

4.2 Chemical synthesis

For the development of greener chemical processes, researchers are trying to use the microfluidic plasma-assisted methods to synthesize chemicals in a catalyst-free manner. With this technology, it is possible to generate energetic reactive species at atmospheric pressure and room temperature within a small spatial dimension. At the same time, operating at the microscale provides a high surface-to-volume ratio, which optimizes mass and energy transfer in the system. The existence of gaseous OH· radicals and their diffusion into the liquid phase has been evidenced and quantified by Michaël et al., where a microfluidic plasma reactor is designed for the generation of polymerization initiators to replace traditionally used chemical initiators. Hydroxyl radicals of 10^{-6} mol/l concentration are detected, making hydroxylation reactions possible. Therefore, the microfluidic plasma can provide a new route for chemical synthesis.

To explore the feasibility of microfluidic plasmas as a synthetic tool in organic chemistry, Julien et al. [30] fabricated a microfluidic chip and linked to a AC high voltage source to generate plasma within microchannels. Meanwhile, liquid cyclohexane and pure O_2 gas was introduced in the microreactor to evaluate the ability of plasma activation for operating oxidation reactions in a controlled way (Figure 8(a-b)). The treatment of liquid cyclohexane with O_2 plasma inside the microchip leads to a partial oxidation of cyclohexane. As a result, a mixture of cyclohexanol, cyclohexanone and cyclohexyl hydroperoxide was detected, with a total selectivity above 70% and

conversion up to 30% (Figure 8(c)). In contrast to other reactions leading to over-oxidations, the results confirm the possibility of activating aliphatic C-H bonds by microfluidic plasma to perform controlled partial oxidation. This is attributed to their unique characteristics, where products are trapped inside the liquid phase. Meanwhile, excited species, ions and radicals can directly react in gas phase or transferred into the adjacent liquid phase to prevent excessive reaction rates. Therefore, microfluidic plasma can provide a new route for chemical synthesis.

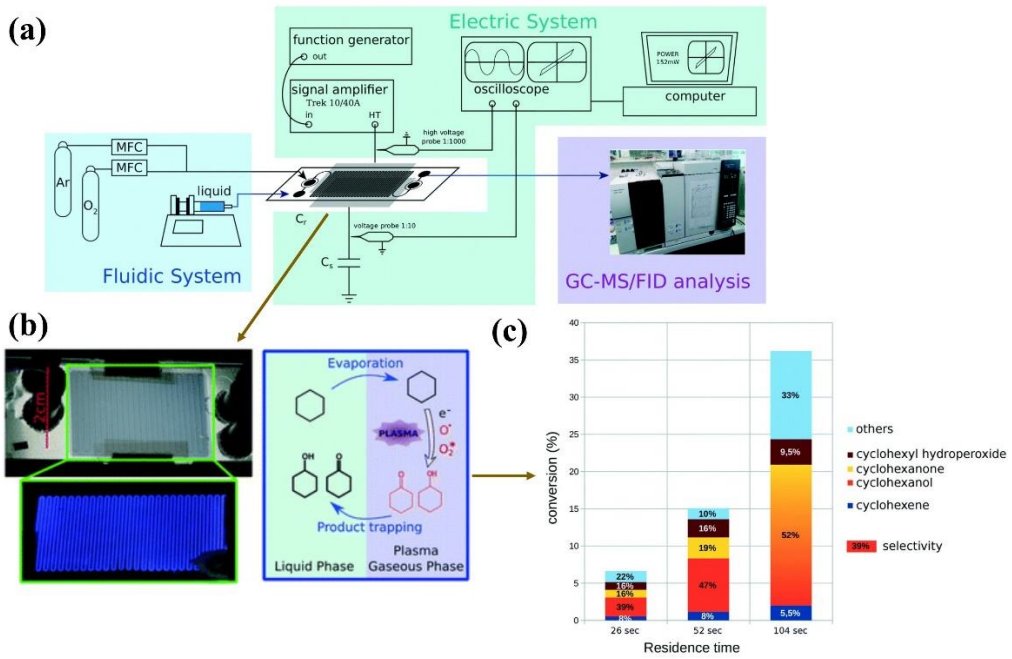

Figure 8. (a) Illustration of the microfluidic plasma setup for the oxidation of cyclohexane; (b) Picture of the microfluidic plasma reactor as well as the oxidative reactions, showing plasma discharges are formed within microchannels; (c) the reaction product of cyclohexane in a microfluidic plasma at various residence times. The number stand for the selectivity of each product. Reprinted with permission from [30], Copyright 2018 The Royal Society of Chemistry.

Another typical example is the production of diamondoids. In the study of Ishii et al. [133], a plasma generated inside a microfluidic reactor was applied to investigate the effect of plasma gas chemistry on the synthesis of diamantine from adamantine. In each experiment, adamantane powder was heated to a certain temperature to obtain desired vapor pressure. Meanwhile, Ar, H_2 and CH_4 were used as the plasma gases to flow adamantine vapors into the microreactor. It is demonstrated that diamantine is successfully synthesized, and the increase of H_2 content from 10% to 40% results in an improvement of diamantine by a factor of four. By contrast, the addition of CH_4 does not have marked

effect on the synthesis, suggesting H_2 is critical for diamondoid synthesis.

4.3 Surface modification

Owing to its easy operation, low-energy consumption, moderate working conditions and highly reactive characteristics, plasma surface treatment has been developed as an effective tool to modify, activate and functionalize materials. The energetic electrons (>1 eV) in non-thermal plasmas can induce molecule excitation, ionization and dissociation, resulting in the breaking and restructuring of chemical bonds [134]. Additionally, since the plasma species only typically have a small penetration depth on the order of 10~100 nm, they are capable of modifying materials surface without changing their bulk properties [135]. Exposure to plasmas can generate polar groups on the surface of polymers, causing changes in their surface energy, electricity properties, hydrophilicity and hydrophobicity. The microscale geometry makes it possible for the accurate modification of the surface of a ultra-small area, like microchips, microchannels, etc.

In the study of Sinton [136], a microfluidic plasma device is developed to achieve liquid actuation in microchannels by the plasma treatment, as shown in Figure 9. Five different microfluidic chips made of PDMS were designed and used in the experiments. Dye solutions for visualization experiments were prepared and filtered with membrane syringe-driven filters. A voltage of 10-50 kV at 4-5 MHz was coupled to the microfluidic chip to form a corona discharge. Once the plasma was formed, the air in the microchannel was ionized. Such instantaneous surface oxidation can cause a change in surface energy at the solid-liquid interface, leading to a reduction in the contact angle. As a result, the liquid is rapidly transported through the channel by capillary action (Figure 9 (b-c)). The contact angle of an ultrapure water droplet on the PDMS surface was found to change from 122° to nearly zero (＜5°) after exposure to the plasma. Furthermore, the average flow velocities were found to increase linearly with the plasma power intensity.

Another representative example based on plasma for microfluidic surface modification is reported by Hsu et al. [137], where an open-surface microfluidic platform was fabricated for liquid transport and mixing (Figure 9(d)). Hexamethyldisiloxane and acrylic acids were used as hydrophobic and hydrophilic precursors respectively and injected into microchannels. After coupling a high voltage

power supply to the system, a plasma jet is formed in the microreactor. Under the plasma treatment, hydrophilic or hydrophobic layers were deposited within microchannels. Thus, the demonstrated method can spatially pattern the surface of microchannels with hydrophobic/hydrophilic areas in real time, and can be applied in microfluidic devices with different materials and geometries. With the development of microfluidics, surface modification of microreactors have become increasingly popular.

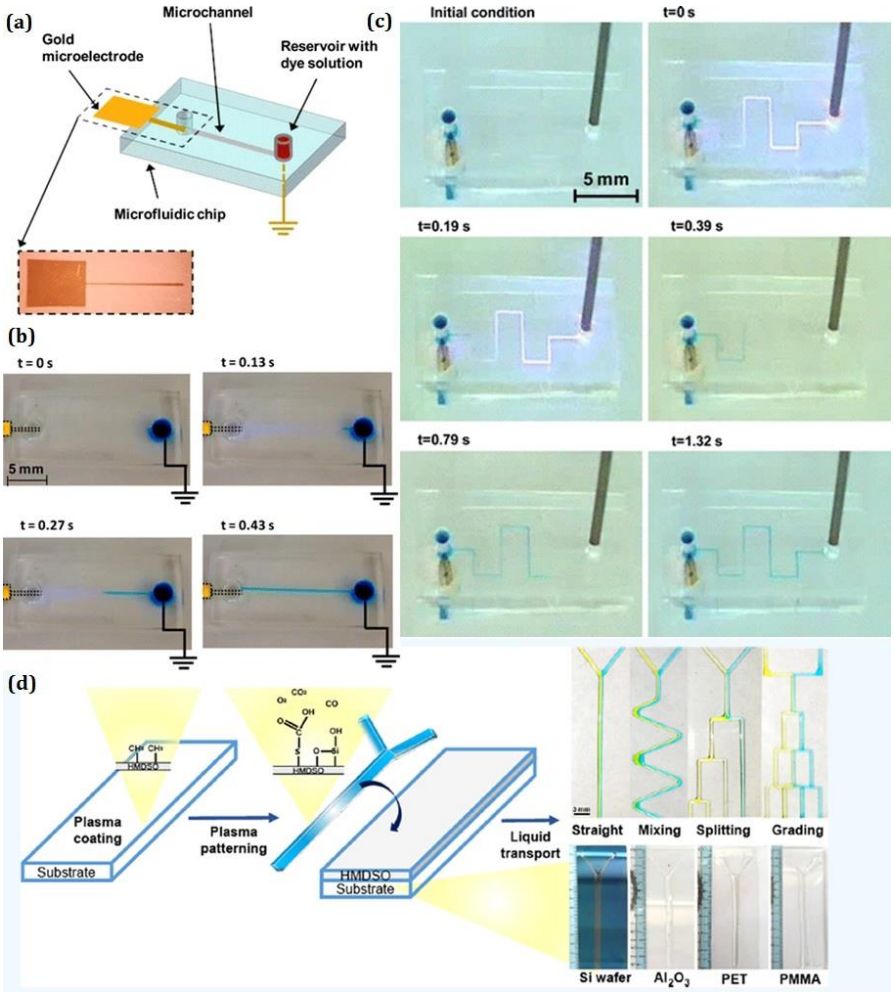

Figure 9. (a) The configuration of the integrated microfluidic plasma device for liquid actuation in microchannels; (b-c) Sequence of images showing liquid actuation in straight/non-straight microchannels at various times. Reprinted with permission from [136], Copyright 2011 Springer-Verlag; (d) Illustration of a microfluidic chip whose surface was patterned by hydrophobic/hydrophilic layers using microfluidic plasmas. Reprinted with permission from [137], Copyright 2019 American Chemical Society.

4.4 Environmental applications

Patinglag et al. studied a dielectric barrier discharge microfluidic plasma reactor, operated at atmospheric pressure, for its potential to treat organic contaminants in water [138]. Microfluidic

microplasma systems when used for water treatment benefit from their inherent characteristics such as a large surface-area-to-volume ratio, good flow control, and being lightweight (allowing use as a portable device). Using a dielectric barrier discharge microplasma, a segmented flow of plasma-gas-liquid slugs is formed. Methylene blue was used to investigate the degradation of organic compounds in the microfluidic microplasma device. The relative degradation rate of methylene blue was influenced by several parameters, including the residence time, type of gas applied, channel depth and flow rate.. The mechanism of degradation is due to the interaction at the interface between plasma and water. As a result, reactive oxygen species (ROS) and UV light are generated at the interface. ROS and UV are the main sources to degrade organic compounds. Recently, in the study of Cullen et al [139], a microjet plasma reactor was demonstrated for the degradation of cefixime antibiotic in water, showing its antibiotic activity was effectively deactivated by the approach, and that no toxic effects were observed toward human cell lines.

4.5 Micro total analysis systems

Micro total analysis systems (μTAS) devices are also commonly referred to as Labs-on-a-Chip (LOC), microchips or microfluidic devices, which focus on separations and the development of a variety of functional elements for sample manipulation and handling [140]. Microfluidic plasma has to ability to integrate complex functions in a microchip to produce truly sample-in/answer-out systems, making them good candidate for the μTAS devices. Li et al. [132] presented a microfluidic plasma chip which consists of reaction zone, gas-liquid separator, collection and UV-Vis detection chamber together for the synthesis of gold nanoparticles and their on-site detection of mercury ions, as shown in Figure 10. $HAuCl_4$ solution was injected into the reaction zone and being reduced to gold nanoparticles under the helium plasma treatment. Afterwards, the gas and liquid phases of the segments were separated by a downstream micro chamber. Due to surface tension and the density difference between the liquid and gas, the liquid part was captured by the lower chamber, while the gas part was extracted by the upper chamber. The collected gold nanoparticles were then injected into the collection chamber for UV-Vis detection of mercury ions. It is shown “reaction-separation-detection” can be integrated into a single chip to form a microfluidic plasma based “chip-factory”, and the

detection limit of Hg^{2+} concentration was found to be 10^{-6} M.

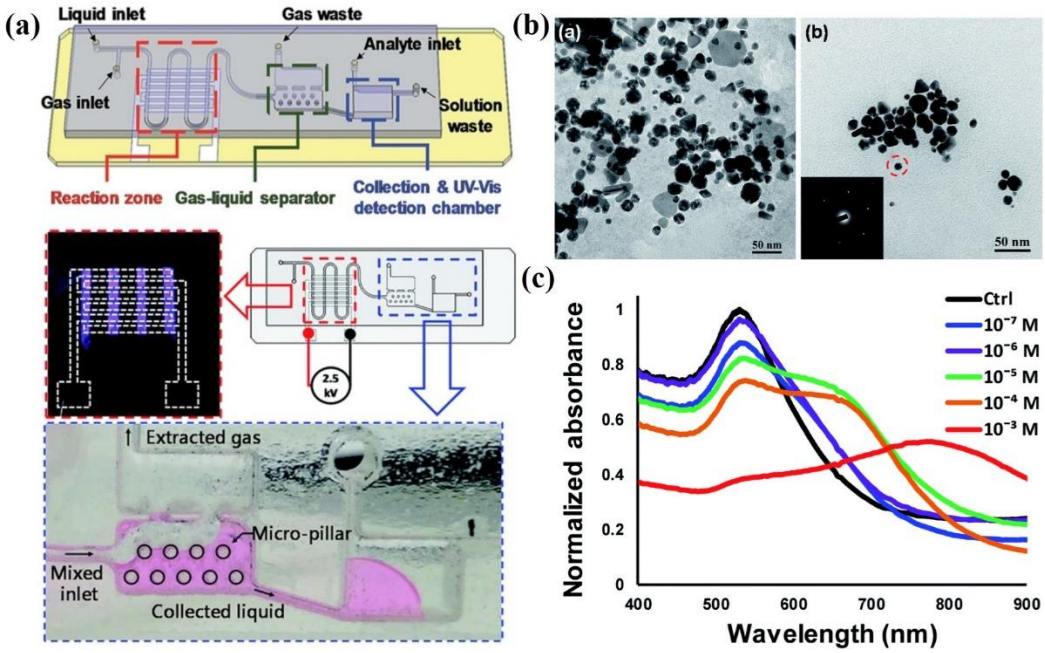

Figure 10. (a) Illustration of the microfluidic plasma based "chip-factory" for the synthesis of Au nanoparticles and the detection of Hg^{2+}; (b) TEM images of the synthesized Au nanoparticles; (c) UV-Vis absorbance spectra for detecting mercury ions at different Hg^{2+} concentrations. Reprinted with permission from [132], Copyright 2018 The Royal Society of Chemistry.

5. Perspectives

We have also pointed out the interplay of microfluidics and plasma in this review. This is a crucial point to investigate in the future. The research needs to show if flow patterns are changed by the presence of plasma. More insight is needed on the fate of the excited species, generated in the plasma gas phase, when they are absorbed into the liquid phase. Also, how plasma might generate excited species directly in the liquid phase. Energy efficiency is thoroughly reported for plasma chemistry with feeding a gas phase only. This needs, however, more investigations, for a biphasic gas-liquid plasma system. The presence of the liquid phase demands to explore the use of homogeneous catalysis. Yet, plasma catalysis was so far the domain of heterogeneous catalysis. Reports about using homogeneous catalysis are rare. Microfluidics offers the opportunity for process integration. Microfluidics and flow chemistry open novel process windows and a considerable part of our past work were related to exploring that [23]. The combination of double-activation, meaning both by plasma and the use of unusual, harsh process conditions (novel process windows) has not been explored so far. Finally, even

basic processes such as mass transfer might be different in the presence of an electric field, which might accelerate the movement of polar and charged species. Driven by its unprecedented advantages, microfluidic plasma is foreseen to undergo technological advancements in a wide range of fields, offering the opportunity for new applications. Here, some contemporary works have been done and we like to exemplify that.

A typical example is highly-sensitive diagnosis using microfluidic plasma chips. Since microfluidic reactors operate at small dimensions, spatial and temporal manipulations of gases, liquids, droplets or bubbles with high accuracy can be achieved. By mixing gas samples with a reference gas (e.g., Ar or He) at a proper ratio, microfluidic plasma devices can be used for gas detection and analysis from the emission spectra. Such device was firstly demonstrated by Fan et al. [142], where a microfluidic plasma chip was developed for optical emission spectroscopy analysis. Characteristic emission peaks of air, Ar, and He were observed; yet more steps are needed to achieve in this way quantitative measurements of gas compositions.

Transfer of lab scale achievements to industrial scale application is a grand challenge. Scale-up of plasma chemistry and especially of microplasma approaches is an open issue; asking for creative solutions. One solution might be numbering up the micro-scale flows. The scale-up of microfluidics has been done up to the industrial scale of several tons or ten-tons per year in the field of pharmaceutical production. Both numbering-up and smart-scale out strategies have been used. Most importantly, before using any of these issues, the productivity has to be maximised, and novel process windows have been proven a viable, industry-taken way. Thus, the recommendation for the scale-up of microfluidic microplasma is to make the best compromise of both approaches in the disciplines. The fluidic smart-scale out approach would likely deteriorate the advantage of the microplasma. Thus, the numbering-up approach might be applied. Then external numbering-up (meaning the multiplication of microdevices) would not suit, as it would ask for a multiplicity of plasma electrodes and their control. This would generate a too complex system. Rather internal numbering-up seems to be a good solution, with many microflows being exposed to a very few joint electrodes; all being operated by one electrical power system.

In addition to the numbering up strategy, another possible solution for the scale-up of microfluidic plasmas is to maximize their operational potentials. Since microplasmas are more reactive than traditional bulk plasmas, the rates of chemical reactions within each microplasma jet are enhanced. Meanwhile, owing to the relatively small dimension of the microplasma jet, the array structure is very compact, making them favoured by industrial or portable applications. For applications like plasma surface modification, microplasma arrays can be used to scan the surface at faster speeds , with enhanced gas flow rates. Despite the above solutions, we admitted that scale-up issues related to microfluidic plasma need be solved by active collaborations from physics, chemistry, materials, chemical and reaction engineering, industrial process, and digital control engineering.

6. Conclusions

As a multidisciplinary research involving microfluidic technology, microengineering, plasma physics, and plasma chemistry, microfluidic plasma has emerged as a novel process window for chemistry and chemical engineering. The integration of microfluidics with plasma may lead to synergistic effects to approach demanding challenges that cannot be solved by plasmas and microfluidics alone, or conventional gas-phase or liquid-phase chemistries. This review focused on the state-of-the-art the recent advances in microfluidic plasmas. Three main discharge configurations have been reviewed, with salient examples provided to show the high degree of design flexibility in the reactor structures. This is followed by the systematic summary of the most commonly applied techniques for characterizing the microfluidic plasmas as well as their applications, aiming to give readers a quick but a reasonably deep insight into this exciting field.

As catalysis is crucial for chemical conversion, a microfluidic plasma-catalysis may have a considerable synergistic potential. The SCOPE project *Fast-modulated plasma for energy intensification*, offers a multi-scale opportunity to synergize non-thermal plasmas with catalysis: nano at the catalyst, micro at the level of modelling plasma generated species, milli at the reactor scale and mega at the plant level [https://cordis.europa.eu/project/id/810182]. With the increasing demand on precision and accuracy process control, faster clinical diagnostics, enhanced portability, and wider operational windows, microfluidic plasmas have great potential to be applied in a wide range of

chemistry and chemical engineering fields.

Acknowledgements

The authors greatly appreciate the funding support from National Natural Science Foundation of China (52004102, 22078125) and Natural Science Foundation of Jiangsu Province (BK20190605). The authors also acknowledge support from the ERC Synergy Grant “Surface-Confined fast modulated plasma for process and energy intensification” (SCOPE) from the European Commission with the Grant No. 810182 as well as the Australian Research Council for partial support.

References

[1] S. Samukawa, M. Hori, S. Rauf, K. Tachibana, P. Bruggeman, G. Kroesen, J.C. Whitehead, A.B. Murphy, A.F. Gutsol, S. Starikovskaia, U. Kortshagen, J.-P. Boeuf, T.J. Sommerer, M.J. Kushner, U. Czarnetzki, N. Mason, The 2012 Plasma Roadmap, J. Phys. D. Appl. Phys. 45 (2012) 253001.
[2] A. Bogaerts, E. Neyts, R. Gijbels, J. Van der Mullen, Gas discharge plasmas and their applications, Spectrochim. Acta - Part B At. Spectrosc. 57 (2002) 609–658.
[3] E.C. Neyts, A.C.T. Van Duin, A. Bogaerts, Insights in the plasma-assisted growth of carbon nanotubes through atomic scale simulations: effect of electric field, J. Am. Chem. Soc. 134 (2012) 1256–1260.
[4] W. Chiang, D. Mariotti, R.M. Sankaran, J.G. Eden, K. (Ken) Ostrikov, Microplasmas for advanced materials and devices, Adv. Mater. (2019) 1905508.
[5] P. Zylka, Evaluation of ozone generation in volume spiral-tubular dielectric barrier discharge source, Energies. 13 (2020) 1199.
[6] L. Lin, H. Xu, H. Gao, X. Zhu, V. Hessel, Plasma-assisted nitrogen fixation in nanomaterials: Fabrication, characterization, and application, J. Phys. D. Appl. Phys. 53 (2020) 133001.
[7] H. Xu, C. He, L. Lin, J. Shen, S. Shang, Direct formation of carbon supported Pt nanoparticles by plasma-based technique, Mater. Lett. 255 (2019) 126532.
[8] R. Snoeckx, A. Bogaerts, Plasma technology-a novel solution for CO_2 conversion?, Chem. Soc. Rev. 46 (2017) 5805–5863.
[9] X. Ma, S. Li, M.R. Lloret, R. Chaudhary, L. Lin, G.V. Rooij, F. Gallucci, G. Rothenberg, N.R. Shiju, V. Hessel, Plasma assisted catalytic conversion of CO_2 and H_2O over Ni/Al_2O_3 in a DBD reactor, Plasma Chem. Plasma Process. 39 (2019) 109–124.
[10] J.R. Toth, N.H. Abuyazid, D.J. Lacks, J.N. Renner, R.M. Sankaran, A plasma-water droplet reactor for process-Intensified, continuous nitrogen fixation at atmospheric pressure, ACS Sustain. Chem. Eng. 8 (2020) 14845–14854.
[11] L. Chandana, P.M.K. Reddy, C. Subrahmanyam, Atmospheric pressure non-thermal plasma jet for the degradation of methylene blue in aqueous medium, Chem. Eng. J. 282 (2015) 116–122.
[12] S. Ojha, A. Fröhling, J. Durek, J. Ehlbeck, B.K. Tiwari, O.K. Schlüter, S. Bußler, Principles and application of cold plasma in food processing, Ref. Modul. Food Sci. 1857 (2020) 1–22.
[13] P.C. Friedman, V. Miller, G. Fridman, A. Fridman, Use of cold atmospheric pressure plasma to treat warts: a potential therapeutic option, Clin. Exp. Dermatol. 44 (2019) 459–461.
[14] K. Ostrikov, E.C. Neyts, M. Meyyappan, Plasma nanoscience: From nano-solids in plasmas to nano-plasmas in solids, Adv. Phys. 62 (2013) 113–224.
[15] V. Vons, Y. Creyghton, A. Schmidt-Ott, Nanoparticle production using atmospheric pressure cold plasma, J. Nanoparticle Res. 8 (2006) 721–728.
[16] K. Ostrikov, Reactive plasmas as a versatile nanofabrication tool, Rev. Mod. Phys. 77 (2005) 489–511.
[17] A.G. A Fridman, A Chirokov, Non-thermal atmospheric pressure discharges, J. Phys. D. Appl. Phys. 38 (2005) R1.
[18] L. Lin, Q. Wang, Microplasma: a new generation of technology for functional nanomaterial synthesis, Plasma Chem. Plasma Process. 35 (2015) 925–962.
[19] K. Jähnisch, V. Hessel, H. Löwe, M. Baerns, Chemistry in microreactors, Angew. Chem. Int. Ed. 43 (2004) 406–446.
[20] P.L. Suryawanshi, S.P. Gumfekar, B.A. Bhanvase, S.H. Sonawane, M.S. Pimplapure, A review on microreactors: Reactor fabrication, design, and cutting-edge applications, Chem. Eng. Sci. 189 (2018) 431–448.
[21] M.B. Plutschack, K. Gilmore, P.H. Seeberger, The Hitchhiker’s guide to flow chemistry, Chem. Rev. 117 (2017) 11796–11893.
[22] M. Guidi, H. Seeberger, K. Gilmore, How to approach flow chemistry, Chem. Soc. Rev. 49 (2020) 8910–8932.
[23] V. Hessel, D. Kralisch, N. Kockmann, Q. Wang, Novel process windows for enabling, accelerating , and uplifting flow chemistry, ChemSusChem. 6 (2013) 746–789.
[24] D. Ott, S. Borukhova, V. Hessel, Life cycle assessment of multi-step rufinamide synthesis – from isolated reactions in

batch to continuous microreactor networks, Green Chem. 18 (2016) 1096–1116.
[25] M. Ko, B. Wyler, C. Aellig, D.M. Roberge, C.A. Hone, C.O. Kappe, Optimization and scale-up of the continuous flow acetylation and nitration of 4‑fluoro-2-methoxyaniline to prepare a key building block of osimertinib, Org. Process Res. Dev. 24 (2020) 2217–2227.
[26] https://en.wikipedia.org/wiki/Assembly_line.
[27] N. Convery, N. Gadegaard, 30 years of microfluidics, Micro Nano Eng. 2 (2019) 76–91.
[28] K. Jähnisch, V. Hessel, H. Löwe, M. Baerns, Chemistry in microstructured reactors, Angew. Chemie - Int. Ed. 43 (2004) 406–446.
[29] X. Yao, Y. Zhang, L. Du, J. Liu, J. Yao, Review of the applications of microreactors, Renew. Sustain. Energy Rev. 47 (2015) 519–539.
[30] J. Wengler, S. Ognier, M. Zhang, E. Levernier, C. Guyon, C. Ollivier, L. Fensterbank, M. Tatoulian, Microfluidic chips for plasma flow chemistry: Application to controlled oxidative processes, React. Chem. Eng. 3 (2018) 930–941.
[31] N. Tsolas, K. Togai, Z. Yin, K. Frederickson, R.A. Yetter, W.R. Lempert, I. V. Adamovich, Plasma flow reactor studies of H_2/O_2/Ar kinetics, Combust. Flame. 165 (2016) 144–153.
[32] A. Fridman, A. Gutsol, Y.I. Cho, Non-thermal atmospheric pressure plasma, 2007.
[33] X. Lu, S. Wu, J. Gou, Y. Pan, An atmospheric-pressure, high-aspect-ratio, cold micro-plasma, Sci. Rep. 4 (2014) 20–24.
[34] J. Hopwood, F. Iza, S. Coy, D.B. Fenner, A microfabricated atmospheric-pressure microplasma source operating in air, J. Phys. D. Appl. Phys. 38 (2005) 1698–1703.
[35] K. Tachibana, Current status of microplasma research, IEEJ Trans. Electr. Electron. Eng. 1 (2006) 145–155.
[36] H. Hilal Kurt, B.G. Salamov, Breakdown phenomenon and electrical process in a microplasma system with InP electrode, Jom. 72 (2020) 651–657.
[37] D. Mariotti, R.M. Sankaran, Microplasmas for nanomaterials synthesis, J. Phys. D. Appl. Phys. 43 (2010) 323001.
[38] M. Zhang, S. Ognier, N. Touati, I. Hauner, C. Guyon, L. Binet, M. Tatoulian, A plasma/liquid microreactor for radical reaction chemistry: An experimental and numerical investigation by EPR spin trapping, Plasma Process. Polym. 15 (2018) e1700188.
[39] Y. Yamanishi, S. Sameshima, H. Kuriki, S. Sakuma, F. Arai, Transportation of mono-dispersed micro-plasma bubble in microfluidic chip under atmospheric pressure, 2013 Transducers eurosensors XXVII: 17th Int. Conf. solid-state sensors, actuators microsystems, transducers eurosensors. 2 (2013) 1795–1798.
[40] O.T. Olabanji, J.W. Bradley, The development and analysis of plasma microfluidic devices, Surf. Coatings Technol. 205 (2011) 516–519.
[41] W.B. Zimmerman, Electrochemical microfluidics, Chem. Eng. Sci. 66 (2011) 1412–1425.
[42] J.H. Lozano-Parada, W.B. Zimmerman, The role of kinetics in the design of plasma microreactors, Chem. Eng. Sci. 65 (2010) 4925–4930.
[43] H. Puliyalil, D. Lašič Jurković, V.D.B.C. Dasireddy, B. Likozar, A review of plasma-assisted catalytic conversion of gaseous carbon dioxide and methane into value-added platform chemicals and fuels, RSC Adv. 8 (2018) 27481–27508.
[44] R. Snoeckx, R. Aerts, X. Tu, A. Bogaerts, Plasma-based dry reforming: A computational study ranging from the nanoseconds to seconds time scale, J. Phys. Chem. C. 117 (2013) 4957–4970.
[45] M.L. Carreon, Plasma catalysis: A brief tutorial, Plasma Res. Express. 1 (2019) 043001.
[46] A. Bogaerts, X. Tu, J.C. Whitehead, G. Centi, L. Lefferts, O. Guaitella, F. Azzolina-Jury, H.H. Kim, A.B. Murphy, W.F. Schneider, T. Nozaki, J.C. Hicks, A. Rousseau, F. Thevenet, A. Khacef, M. Carreon, The 2020 plasma catalysis roadmap, J. Phys. D. Appl. Phys. 53 (2020) 443001.
[47] J.C. Whitehead, Plasma-catalysis: Is it just a question of scale?, Front. Chem. Sci. Eng. 13 (2019) 264–273.
[48] L. Lin, S.A. Starostin, S. Li, V. Hessel, Synthesis of metallic nanoparticles by microplasma, Phys. Sci. Rev. 3 (2018) 1–34.
[49] J. Benedikt, M. Mokhtar Hefny, A. Shaw, B.R. Buckley, F. Iza, S. Schäkermann, J.E. Bandow, The fate of plasma-generated oxygen atoms in aqueous solutions: Non-equilibrium atmospheric pressure plasmas as an efficient source of atomic O(aq), Phys. Chem. Chem. Phys. 20 (2018) 12037–12042.
[50] J. Šimončicová, S. Kryštofová, V. Medvecká, K. Ďurišová, B. Kaliňáková, Technical applications of plasma treatments: current state and perspectives, Appl. Microbiol. Biotechnol. 103 (2019) 5117–5129.
[51] M. Laroussi, Cold plasma in medicine and healthcare: the new frontier in low temperature plasma applications, Front. Phys. 8 (2020) 74.
[52] C. Dechthummarong, Characterizations of electrical discharge plasma in air micro/nano-bubbles water mixture, Int. J. Plasma Environ. Sci. Technol. 12 (2019) 64–68.
[53] W. Luc, F. Jiao, Synthesis of nanoporous metals, oxides, carbides, and sulfides: beyond nanocasting, Acc. Chem. Res. 49 (2016) 1351–1358.
[54] M. Gharib, S. Mendoza, M. Rosenfeld, M. Beizai, F.J. Alves Pereira, Toroidal plasmoid generation via extreme hydrodynamic shear, PNAS. 114 (2017) 12657–12662..
[55] A. Dzimitrowicz, A. Bielawska-Pohl, P. Jamroz, J. Dora, A. Krawczenko, G. Busco, C. Grillon, C. Kieda, A. Klimczak, D. Terefinko, A. Baszczynska, P. Pohl, Activation of the normal human skin cells by a portable dielectric barrier discharge-based reaction-discharge system of a defined gas temperature, Plasma Chem. Plasma Process. 40 (2020) 79–97.
[56] S. Kuo, Air plasma spray for first aid, Open J. Emerg. Med. 4 (2016) 69–82.
[57] S.W. Lee, R.M. Sankaran, Direct writing via electron-driven reactions, Mater. Today. 16 (2013) 117–122.
[58] A. Thiha, F. Ibrahim, S. Muniandy, M.J. Madou, Microplasma direct writing for site-selective surface functionalization of carbon microelectrodes, Microsystems Nanoeng. 5 (2019) 62.

[59] L. Lin, S.A. Starostin, Q. Wang, V. Hessel, An atmospheric pressure microplasma process for continuous synthesis of titanium nitride nanoparticles, Chem. Eng. J. 321 (2017) 447-457.
[60] B. Zhang, Z. Fang, M. Wan, H. Wan, K. (Ken) Ostrikov, Jet-to-jet interactions in atmospheric-pressure plasma jet arrays for surface processing, Plasma Process. Polym. 15 (2018) 1700114.
[61] M. Ghasemi, P. Olszewski, J.W. Bradley, J.L. Walsh, Interaction of multiple plasma plumes in an atmospheric pressure plasma jet array, J. Phys. D. Appl. Phys. 46 (2013) 052001.
[62] F. Liu, M. Cai, B. Zhang, Z. Fang, C. Jiang, K. (Ken) Ostrikov, Hydrophobic surface modification of polymethyl methacrylate by two-dimensional plasma jet array at atmospheric pressure, J. Vac. Sci. Technol. A. 36 (2018) 061302.
[63] Z. Cao, J.L. Walsh, M.G. Kong, Atmospheric plasma jet array in parallel electric and gas flow fields for three-dimensional surface treatment, Appl. Phys. Lett. 94 (2009) 021501.
[64] D.Y. Kim, S.J. Kim, H.M. Joh, T.H. Chung, Characterization of an atmospheric pressure plasma jet array and its application to cancer cell treatment using plasma activated medium, Phys. Plasmas. 25 (2018) 073505.
[65] P.P. Sun, E.M. Araud, C. Huang, Y. Shen, G.L. Monroy, S. Zhong, Z. Tong, S.A. Boppart, J.G. Eden, T.H. Nguyen, Disintegration of simulated drinking water biofilms with arrays of microchannel plasma jets, Npj Biofilms Microbiomes. 4 (2018) 24.
[66] Y. Sui, A. Hess-dunning, P. Wei, E. Pentzer, R.M. Sankaran, C.A. Zorman, Electrically conductive, reduced graphene oxide structures fabricated by inkjet printing and low temperature plasma reduction, Adv. Mater. Technol. 4 (2019) 1900834.
[67] S. Ghosh, E. Klek, C.A. Zorman, R. Mohan Sankaran, Microplasma-induced in situ formation of patterned, stretchable electrical conductors, ACS Macro Lett. 6 (2017) 194–199.
[68] S. Reuter, T. Von Woedtke, K.D. Weltmann, The kINPen - A review on physics and chemistry of the atmospheric pressure plasma jet and its applications, J. Phys. D. Appl. Phys. 51 (2018) 233001.
[69] H. Xu, Y. Li, L. Lin, J. Shen, X. Chen, Study on the synthesis and compounding performance of C21 dibasic acid potassium, J. Surfactants Deterg. 23 (2020) 855–862.
[70] H. Ding, L. Lin, D. Gu, S. Shang, Synthesis and surface modification of submicron $BaTiO_3$ powders via a facile surfactant-assisted method, Ceram. Int. 46 (2020) 22040–22048.
[71] K. Ishikawa, Plasma Diagnostics, in: Cold Plasma Food Agric. Fundam. Appl., Elsevier Inc., 2016: 117–141.
[72] P. Bruggeman, U. Czarnetzki, K. Tachibana, Diagnostics of atmospheric pressure microplasmas, J. Phys. D. Appl. Phys. 46 (2013).
[73] C.S. Wong, R. Mongkolnavin, Plasma diagnostic techniques, in: SpringerBriefs Appl. Sci. Technol., Springer, Singapore, 2015: 49–98.
[74] I. Choi, C. Chung, S. Youn Moon, Electron density and electron temperature measurement in a bi-Maxwellian electron distribution using a derivative method of Langmuir probes, Phys. Plasmas. 20 (2013) 083508.
[75] S. Kumari, A. Kushwaha, A. Khare, Spatial distribution of electron temperature and ion density in laser induced ruby (Al_2O_3:Cr^{3+}) plasma using Langmuir probe, J. Instrum. 7 (2012) C05017.
[76] K.G. Xu, S.J. Doyle, Measurement of atmospheric pressure microplasma jet with Langmuir probes, J. Vac. Sci. Technol. A Vacuum, Surfaces, Film. 34 (2016) 051301.
[77] L.M. Blair, K.G. Xu, Langmuir probe diagnostics of an atmospheric-pressure microplasma, 46th AIAA Plasmadynamics Lasers Conf. (2015) 1–15.
[78] R. Brandenburg, Dielectric barrier discharges: progress on plasma sources and on the understanding of regimes and single filaments, Plasma Sources Sci. Technol. 26 (2017) 053001.
[79] F. Peeters, T. Butterworth, Electrical diagnostics of dielectric barrier discharges, Atmos. Press. Plasma - from Diagnostics to Appl., IntechOpen, 2019.
[80] O. Ogunyinka, A. Wright, G. Bolognesi, F. Iza, H.C.H. Bandulasena, An integrated microfluidic chip for generation and transfer of reactive species using gas plasma, Microfluid. Nanofluidics. 24 (2020) 13.
[81] K.W. Jo, M.G. Kim, S.M. Shin, J.H. Lee, Microplasma generation in a sealed microfluidic glass chip using a water electrode, Appl. Phys. Lett. 92 (2008) 7–10.
[82] O. Olabanji, O. Olabanji, O. Olabanji, The study and characterisation of plasma microfluidic devices, 2012. The University of Liverpool Repository.
[83] C. Ishii, S. Stauss, K. Kuribara, K. Urabe, T. Sasaki, K. Terashima, Atmospheric pressure synthesis of diamondoids by plasmas generated inside a microfluidic reactor, Diam. Relat. Mater. 59 (2015) 40–46.
[84] S. Stauss, C. Ishii, D.Z. Pai, K. Urabe, K. Terashima, Diamondoid synthesis in atmospheric pressure adamantane-argon-methane-hydrogen mixtures using a continuous flow plasma microreactor, Plasma Sources Sci. Technol. 23 (2014) 035016.
[85] H. Yoshiki, T. Sasaki, T. Mitsui, Inner-wall modification of a commercial polymeric microfluidic chip using pulsed He/O_2 and Ar/O_2 μplasmas, Jpn. J. Appl. Phys. 57 (2018) 126202.
[86] L. Lin, S.A. Starostin, X. Ma, S. Li, S.A. Khan, V. Hessel, Facile synthesis of lanthanide doped yttria nanophosphors by a simple microplasma-assisted process, React. Chem. Eng. 4 (2019) 891–898.
[87] K.H. Schoenbach, K. Becker, 20 years of microplasma research: a status report, Eur. Phys. J. D. 70 (2016) 29.
[88] S.Y. Songbai W, Guangjiu L, Dongping L, Balmer H_α , H_β and H_γ spectral lines intensities in high-power RF hydrogen plasmas, Plasma Sci Technol. 16 (2014) 219–222.
[89] G. Dilecce, Optical spectroscopy diagnostics of discharges at atmospheric pressure, Plasma Sources Sci. Technol. 23 (2014) 015011.
[90] B.S. Sommers, S.F. Adams, A comparison of gas temperatures measured by ultraviolet laser scattering in atmospheric plasma sources, J. Phys. D. Appl. Phys. 48 (2015) 485202.

[91] K. Urabe, H. Muneoka, S. Stauss, K. Terashima, Development of near-infrared laser heterodyne interferometry for diagnostics of electron and gas number densities in microplasmas, Appl. Phys. Express. 6 (2013) 126101.
[92] K. Urabe, H. Muneoka, S. Stauss, K. Terashima, Microscopic heterodyne interferometry for determination of electron density in high-pressure microplasma, Plasma Sources Sci. Technol. 23 (2014) 064007.
[93] K. Hattori, Y. Noguchi, A. Ando, M. Inutake, A multi-reflection type visible-laser interferometer for high density plasma measurements, Plasma Fusion Res. 2 (2007) S1048.
[94] W. Lei, V. Motto-ros, M. Boueri, Q. Ma, D. Zhang, L. Zheng, H. Zeng, J. Yu, Spectrochimica Acta Part B Time-resolved characterization of laser-induced plasma from fresh potatoes, Spectrochim. Acta Part B At. Spectrosc. 64 (2009) 891–898.
[95] P.J. Bruggeman, M.J. Kushner, B.R. Locke, et al., Plasma–liquid interactions: a review and roadmap, Plasma Sources Sci. Technol. 25 (2016) 053002.
[96] Hansjoachim Bluhm, Pulsed power systems: principles and applications, Springer-Verlag Berlin Heidelberg, 2006.
[97] D. Marinov, N.S.J. Braithwaite, Power coupling and electrical characterization of a radio-frequency micro atmospheric pressure plasma jet, Plasma Sources Sci. Technol. 23 (2014) 062005.
[98] S. Hofmann, A.F.H. Van Gessel, T. Verreycken, P. Bruggeman, Power dissipation, gas temperatures and electron densities of cold atmospheric pressure helium and argon RF plasma jets, Plasma Sources Sci. Technol. 20 (2011) 065010.
[99] P. Bruggeman, D. Schram, M.Á. González, R. Rego, M.G. Kong, C. Leys, Characterization of a direct dc-excited discharge in water by optical emission spectroscopy, Plasma Sources Sci. Technol. 18 (2009) 025017.
[100] M. Ivković, S. Jovićević, N. Konjević, Low electron density diagnostics: Development of optical emission spectroscopic techniques and some applications to microwave induced plasmas, Spectrochim. Acta - Part B At. Spectrosc. 59 (2004) 591–605.
[101] K. Muraoka, A. Kono, Laser thomson scattering for low-temperature plasmas, J. Phys. D. Appl. Phys. 44 (2011) 043001.
[102] L. Taghizadeh, A. Nikiforov, R. Morent, J. Van Der Mullen, C. Leys, Determination of the electron temperature of atmospheric pressure argon plasmas by absolute line intensities and a collisional radiative model, Plasma Process. Polym. 11 (2014) 777–786.
[103] P.J. Bruggeman, N. Sadeghi, D.C. Schram, V. Linss, Gas temperature determination from rotational lines in non-equilibrium plasmas: A review, Plasma Sources Sci. Technol. 23 (2014) 023001.
[104] J. Schäfer, R. Foest, S. Reuter, T. Kewitz, J. Šperka, K.D. Weltmann, Laser schlieren deflectometry for temperature analysis of filamentary non-thermal atmospheric pressure plasma, Rev. Sci. Instrum. 83 (2012) 103506.
[105] S.M. Starikovskaia, K. Allegraud, O. Guaitella, A. Rousseau, On electric field measurements in surface dielectric barrier discharge, J. Phys. D. Appl. Phys. 43 (2010) 124007.
[106] T. Ito, K. Kobayashi, S. Mueller, D. Luggenhölscher, U. Czarnetzki, S. Hamaguchi, Electric field measurement in an atmospheric or higher pressure gas by coherent Raman scattering of nitrogen, J. Phys. D. Appl. Phys. 42 (2009) 092003.
[107] D. Riès, G. Dilecce, E. Robert, P.F. Ambrico, S. Dozias, J.M. Pouvesle, LIF and fast imaging plasma jet characterization relevant for NTP biomedical applications, J. Phys. D. Appl. Phys. 47 (2014) 275401.
[108] M.P. Arroyo, R.K. Hanson, Absorption measurements of water-vapor concentration, temperature, and line-shape parameters using a tunable InGaAsP diode laser, Appl. Opt. 32 (1993) 6104–6116.
[109] C.M. Penney, M. Lapp, Raman-scattering cross sections for water vapor, J. Opt. Soc. Am. 66 (1976) 422–425.
[110] A.F.H. Van Gessel, E.A.D. Carbone, P.J. Bruggeman, J.J.A.M. Van Der Mullen, Laser scattering on an atmospheric pressure plasma jet: Disentangling Rayleigh, Raman and Thomson scattering, Plasma Sources Sci. Technol. 21 (2012) 015003.
[111] M. Dünnbier, A. Schmidt-Bleker, J. Winter, M. Wolfram, R. Hippler, K.D. Weltmann, S. Reuter, Ambient air particle transport into the effluent of a cold atmospheric-pressure argon plasma jet investigated by molecular beam mass spectrometry, J. Phys. D. Appl. Phys. 46 (2013) 435203.
[112] J. Benedikt, A. Hecimovic, D. Ellerweg, A. Von Keudell, Quadrupole mass spectrometry of reactive plasmas, J. Phys. D. Appl. Phys. 45 (2012) 403001.
[113] H.F. Döbele, T. Mosbach, K. Niemi, V. Schulz-Von Der Gathen, Laser-induced fluorescence measurements of absolute atomic densities: concepts and limitations, Plasma Sources Sci. Technol. 14 (2005) S31–S41.
[114] B.T.J. Van Ham, S. Hofmann, R. Brandenburg, P.J. Bruggeman, In situ absolute air, O_3 and NO densities in the effluent of a cold RF argon atmospheric pressure plasma jet obtained by molecular beam mass spectrometry, J. Phys. D. Appl. Phys. 47 (2014) 224013.
[115] S.G. Belostotskiy, V.M. Donnelly, D.J. Economou, N. Sadeghi, Spatially resolved measurements of argon metastable ($1s_5$) density in a high pressure microdischarge using diode laser absorption spectroscopy, IEEE Trans. Plasma Sci. 37 (2009) 852–858.
[116] G.D. Stancu, M. Janda, F. Kaddouri, D.A. Lacoste, C.O. Laux, Time-resolved CRDS measurements of the $N_2(A^3\Sigma_u^+)$ density produced by nanosecond discharges in atmospheric pressure nitrogen and air, J. Phys. Chem. A. 114 (2010) 201–208.
[117] Y. Sakiyama, D.B. Graves, H. Chang, T. Shimizu, G.E. Morfill, Plasma chemistry model of surface microdischarge in humid air and dynamics of reactive neutral species, J. Phys. D. Appl. Phys. 45 (2012) 425201.
[118] J. Winter, H. Tresp, M.U. Hammer, S. Iseni, S. Kupsch, A. Schmidt-Bleker, K. Wende, M. Dunnbier, K. Masur, K.D. Weltmann, S. Reuter, Tracking plasma generated H_2O_2 from gas into liquid phase and revealing its dominant impact on human skin cells, J. Phys. D. Appl. Phys. 47 (2014) 285401.
[119] P. Bruggeman, F. Iza, D. Lauwers, Y.A. Gonzalvo, Mass spectrometry study of positive and negative ions in a capacitively coupled atmospheric pressure RF excited glow discharge in He–water mixtures, J. Phys. D. Appl. Phys. 43

(2010) 012003.
[120] H. Search, C. Journals, A. Contact, M. Iopscience, I.P. Address, Behavior of N_2^+ ions in He microplasma jet at atmospheric pressure measured by laser induced fluorescence spectroscopy, Appl. Phys. Express. 1 (2008) 066004.
[121] T.H. Ahn, K. Nakamura, H. Sugai, Negative ion measurements and etching in a pulsed-power inductively coupled plasma in chlorine, Plasma Source Sci. Technol. 5 (1996) 139–144.
[122] R. Akçan, H.C. Aydogan, M.Ş. Yildirim, B. Taştekin, N. Sağlam, Nanotoxicity: A challenge for future medicine, Turkish J. Med. Sci. 50 (2020) 1180–1196.
[123] L. Lin, S.A. Starostin, V. Hessel, Q. Wang, Synthesis of iron oxide nanoparticles in microplasma under atmospheric pressure, Chem. Eng. Sci. 168 (2017) 360–371.
[124] L. Lin, S. Li, V. Hessel, S.A. Starostin, R. Lavrijsen, W. Zhang, Synthesis of Ni nanoparticles with controllable magnetic properties by atmospheric pressure microplasma assisted process, AIChE J. 64 (2018) 1540–1548.
[125] L. Lin, S.A. Starostin, S. Li, S.A. Khan, V. Hessel, Synthesis of yttrium oxide nanoparticles via a facile microplasma-assisted process, Chem. Eng. Sci. 178 (2018) 157–166.
[126] L.L. Lin, X.T. Ma, S.A. Starostin, S.R. Li, V. Hessel, J. Shen, S.M. Shang, H.J. Xu, Color-tunable Eu^{3+} and Tb^{3+} co-doped nanophosphors synthesis by plasma-assisted method, ChemistrySelect. 4 (2019) 4278–4286.
[127] L. Lin, X. Ma, S. Li, M. Wouters, V. Hessel, Plasma-electrochemical synthesis of europium doped cerium oxide nanoparticles, Front. Chem. Sci. Eng. 13 (2019) 501–510.
[128] X. Ma, S. Li, V. Hessel, L. Lin, S. Meskers, F. Gallucci, Synthesis of N-doped carbon dots via a microplasma process, Chem. Eng. Sci. 220 (2020) 115648.
[129] A.U. Haq, S. Askari, A. McLister, S. Rawlinson, J. Davis, S. Chakrabarti, V. Svrcek, P. Maguire, P. Papakonstantinou, D. Mariotti, Size-dependent stability of ultra-small α-/β-phase tin nanocrystals synthesized by microplasma, Nat. Commun. 10 (2019) 817.
[130] Z. Machala, B. Tarabová, D. Sersenová, M. Janda, K. Hensel, Chemical and antibacterial effects of plasma activated water: Correlation with gaseous and aqueous reactive oxygen and nitrogen species, plasma sources and air flow conditions, J. Phys. D. Appl. Phys. 52 (2019) 034002.
[131] P. Rumbach, D.M. Bartels, R.M. Sankaran, D.B. Go, The solvation of electrons by an atmospheric-pressure plasma, Nat. Commun. 6 (2015) 7248.
[132] D.E. Li, C.H. Lin, Microfluidic chip for droplet-based AuNP synthesis with dielectric barrier discharge plasma and on-chip mercury ion detection, RSC Adv. 8 (2018) 16139–16145.
[133] C. Ishii, S. Stauss, K. Kuribara, K. Urabe, T. Sasaki, K. Terashima, Atmospheric pressure synthesis of diamondoids by plasmas generated inside a microfluidic reactor, Diam. Relat. Mater. 59 (2015) 40–46.
[134] S. Mathioudaki, C.R. Vandenabeele, R. Tonneau, A. Pflug, J. Tennyson, S. Lucas, Plasma polymerization of cyclopropylamine in a low-pressure cylindrical magnetron reactor: A PIC-MC study of the roles of ions and radicals, J. Vac. Sci. Technol. A. 38 (2020) 033003.
[135] K. Kyzioł, Ł. Kaczmarek, G. Brzezinka, A. Kyzioł, Structure, characterization and cytotoxicity study on plasma surface modified Ti-6Al-4V and γ-TiAl alloys, Chem. Eng. J. 240 (2014) 516–526.
[136] C. Escobedo, D. Sinton, Microfluidic liquid actuation through ground-directed electric discharge, Microfluid. Nanofluidics. 11 (2011) 653–662.
[137] S.T. Wu, C.Y. Huang, C.C. Weng, C.C. Chang, B.R. Li, C.S. Hsu, Rapid prototyping of an open-surface microfluidic platform using wettability-patterned surfaces prepared by an atmospheric-pressure plasma jet, ACS Omega. 4 (2019) 16292–16299.
[138] L. Patinglag, D. Sawtell, A. Iles, L.M. Melling, K.J. Shaw, A microfluidic atmospheric−pressure plasma reactor for water treatment, Plasma Chem. Plasma Process. 39 (2019) 561–575.
[139] T. Zhang, R. Zhou, P. Wang, A. Mai-Prochnow, R. McConchie, W. Li, R. Zhou, E.W. Thompson, K. Ostrikov, P.J. Cullen, Degradation of cefixime antibiotic in water by atmospheric plasma bubbles: performance, degradation pathways and toxicity evaluation, Chem. Eng. J. (2020) 127730.
[140] C.T. Culbertson, T.G. Mickleburgh, S.A. Stewart-james, A. Kathleen, M. Pressnall, Micro total analysis systems: fundamental advances and biological applications, Anal. Chem. 86 (2014) 95–118.
[141] T. Kárpáti, E. Holczer, J. Ferencz, A.E. Pap, P. Fürjes, In-situ surface modification of microfluidic channels by integrated plasma source, Procedia Eng. 87 (2014) 484–487.
[142] S.K. Fan, Y.T. Shen, L.P. Tsai, C.C. Hsu, F.H. Ko, Y.T. Cheng, Atmospheric-pressure microplasma in dielectrophoresis-driven bubbles for optical emission spectroscopy, Lab Chip. 12 (2012) 3694–3699.